Summer 2011

Towards on-line voltage stability assessment using synchrophasors

Himanshu Subandhu Hirlekar

Department:

TOWARDS ON-LINE VOLTAGE STABILITY ASSESSMENT USING SYNCHROPHASORS

by

HIMANSHU SUBANDHU HIRLEKAR

A THESIS

Presented to the Faculty of the Graduate School of the

MISSOURI UNIVERSITY OF SCIENCE AND TECHNOLOGY

In Partial Fulfillment of the Requirements for the Degree

MASTER OF SCIENCE IN ELECTRICAL ENGINEERING

2011

Approved by

Dr. Badrul H. Chowdhury, Advisor
Dr. Mehdi Ferdowsi
Dr. Jonathan Kimball

ABSTRACT

Voltage instability has become a growing concern in the operation of power systems in recent years. The reason is that power systems all over are being operated with reduced margins because of increased demand exacerbated by a general reluctance to invest in improvement of the electric grid infrastructure. Until recently it was difficult to predict voltage instability in the on-line environment. However, advances in technology has made possible the on-line monitoring and assessment of voltage stability. Synchrophasors is a relatively new technology in the field of power systems which allows system operators to monitor the system conditions at specific measurement locations of the network. Synchrophasors measure voltage and current phasors with accurate time stamping with respect to Global Positioning System (GPS) clock reference. Because of the accurate time stamping, it becomes possible to compare the phasors in time. A novel voltage stability prediction algorithm using synchrophasors is proposed in this thesis. Synchrophasor data is used to perform a fast state estimation of the system. This is a departure from conventional SCADA-based state estimation. The traditional method of VQ analysis for voltage stability is put to use in this algorithm to estimate the voltage stability margin. Since we are incorporating the synchrophasor information for which the data refresh rate is fast, the algorithm being developed is proposed for on-line stability assessment. The algorithm is tested on the CIGRE 10-bus system. The results are validated using the well-known modal analysis method.

ACKNOWLEDGEMENTS

I would like to express my sincere gratitude and appreciation to my advisor, Dr. Badrul H. Chowdhury, for providing me the opportunity to pursue this research. I sincerely appreciate his invaluable advice, guidance, supervision and encouragement throughout my Master's program and with my research. He has been a continuous source of motivation and has helped me to develop my skills. I dedicate this thesis to him.

I would like to thank Dr. Mehdi Ferdowsi and Dr. Jonathan Kimball for their time and effort in serving as committee members and also for all the valuable information they imparted in the courses that I have had with them.

Lastly, I am obliged to my parents, and my friends who have been very supportive throughout my studies offering encouragement. Without their support, I would not have achieved my Master's study.

TABLE OF CONTENTS

Page

APPENDICES

LIST OF ILLUSTRATIONS

LIST OF TABLES

Table **Page**

NOMENCLATURE

Symbol	Description
SVP	Synchrophasor Vector Processor
LTC	Load Tap Changing
AC	Alternating Current
VSI	Voltage Stability Index
COA	Centre of Angles
GPS	Global Positioning System
PMU	Phasor Measurement Unit

1. INTRODUCTION

1.1 MOTIVATION

With an ever increasing demand and without much improvement in the grid infrastructure, voltage instability has posed a looming threat in the operation of power systems in recent years. Deregulation of power systems all around the globe is forcing utilities to make efficient use of the transmission infrastructure available. As a result, power transfers across transmission lines have increased and many systems are operating with reduced voltage stability margins. Many cases of voltage instability have been reported in the past several decades all round the world [1]. These incidents have occurred because of the system operating with very low margins under normal conditions. As such, work is progressing in detecting voltage instability in real time and developing strategies to mitigate such instability once it has been detected. With the use of synchrophasors, it is possible to compute voltage security margins and take actions accordingly in real time. The objective of this thesis is to compute voltage stability margins mostly using synchrophasors. Traditional methods of state estimation and V-Q analysis for voltage stability assessment are used to compute the available margin before voltage collapse.

1.2 SYNCHROPHASORS AND SYNCHROPHASOR APPLICATIONS

Synchronized phasors or synchrophasors technology are starting to be deployed by utilities around the world. The current applications of synchrophasors are limited and they are mainly used for monitoring the system state and for post-event analysis. But with advances in technology, they can be used for real-time control and for remedial actions.

The synchrophasor technology provides a method of representing the phasors in power system to an absolute time reference [2]. Synchrophasors measure voltage and current phasors with accurate time stamping using a GPS clock. The accurate time stamping allows one to compare two or more phasors at a given instant, thus making it possible to study the state of the system.

Some recent applications of synchrophasors are described below:

SCADA-based voltage control of a large area is not possible since these systems are static data acquisition systems and lack real-time data acquisition capability for the precise control of a wide area. Synchrophasors can solve this problem by time-stamping the data and then aligning the data to a common time reference for processing. A Synchrophasor Vector Processor (SVP) may be used in wide-area control. The SVP aligns the data received from the field devices, assesses the complete system voltage profile and then sends optimized voltage set points to individual Load Tap Changing (LTC) transformer controllers for a more precise wide area control [3].

Reference [2] presents a case study of governor mode control in Abbott Pharmaceuticals using synchrophasors. Abbott Pharmaceuticals have their own generation and have upgraded their distribution system to improve reliability. The new system is designed such that critical plant loads are islanded by detecting disturbances on the grid. For such a system to function properly, it is essential to find out when the cogeneration is coupled to the utility grid. When the cogeneration is connected to the grid, the frequency is controlled by the grid and the generator power is controlled by the governor. In islanded mode, the governor is switched to isochronous mode to control the frequency. When non-time aligned data is used to detect synchronism, it can give false

detection since the two systems can operate at nearly the same frequency. Thus including angle information along with frequency solved the problem. Traditional monitoring systems are not capable of handling angle information due to lack of a common time reference. The new system using synchrophasors makes use of the angle information along with frequency measurement to detect synchronism and thus to change the governor settings. The relay logic to detect synchronism is shown in Figure 1.1:

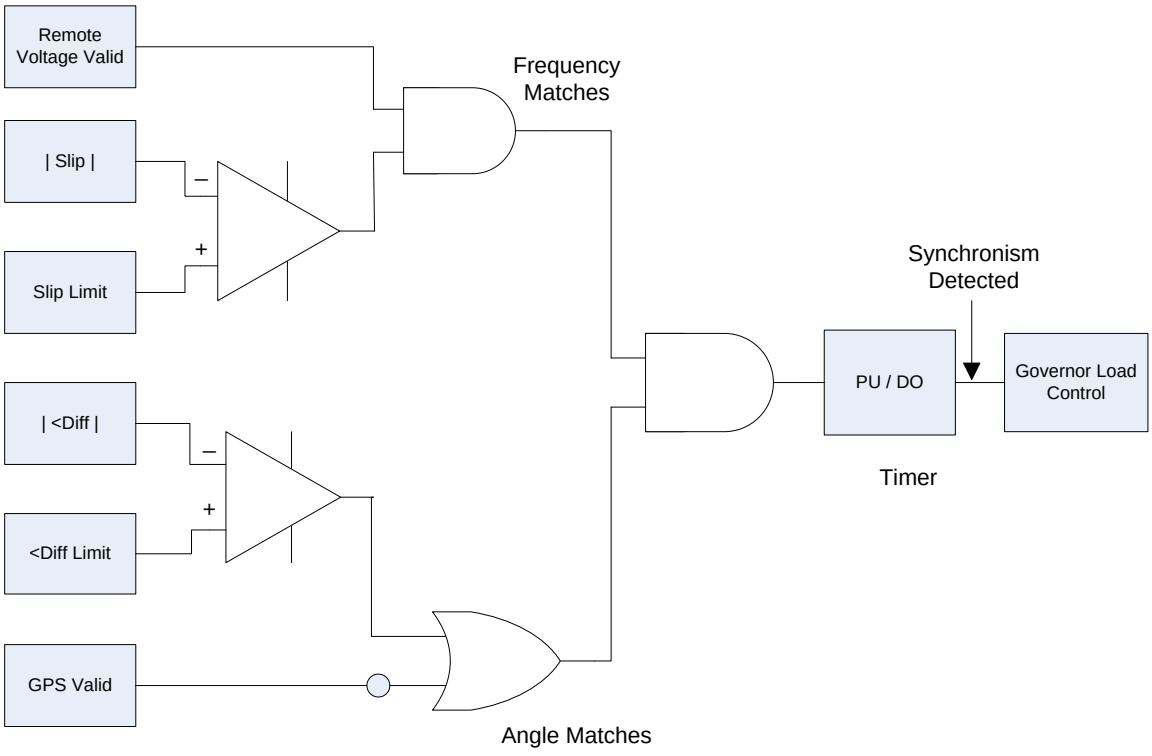

Figure 1.1 Synchronism detection logic [3]

Synchrophasors have been used for real time detection of angle instability [4]. The angle instability is detected by visualizing the phase angles of the buses. The angle instability algorithm analyzes the stability in two stages – a) It computes angle stability for each area. b) It computes angle stability for the complete system. The principle is the same in each stage that is the concept of Centre of Angles (COA) is used in both cases. It computes the COA`s for each area and for the entire system. Then heuristic rules are applied to detect angle instability. If the COA of Area i continuously increases beyond a specified limit from the COA of the entire system, it is interpreted that Area i is moving towards separation from the rest of the system. Similar is the case if the COA of Area i continuously decreases beyond the threshold from COA of the system.

References [5], [6], [7] and [8] describe various other applications of synchrophasors for wide area monitoring, protection and control. Reference [5] describes the application of synchrophasors for service restoration, voltage optimization, power factor correction and automatic network reconfiguration for faults. It discusses the use of synchrophasor information for achieving the above control objectives. Synchrophasors have been put to use in a monitoring and warning system and for a remedial action scheme (RAS). Reference [6] gives an overview of the remedial action scheme using synchrophasors and also discusses how it is different from the traditional RAS scheme. Reference [7] discusses the synchrophasor applications in protection based on synchrophasor, wide area disturbance recording, wide-area frequency monitoring, etc. Strategies for deployment of phasor measurement units (PMU) for wide area monitoring, protection and control are described in reference [8].

1.3 OUTLINE OF THESIS

This thesis is organized into four sections. The first section describes the motivation behind this thesis, synchrophasors and real world applications developed using synchrophasors.

The second section throws light on the work done in the field of voltage stability and state estimation using synchrophasors. It presents two cases studies related to real world applications of synchrophasors to determine voltage stability and also describes the state estimation algorithm using synchrophasors.

The third section describes the synchrophasor data obtained from PowerWorld by running transient analysis tool and the processing necessary for removing bad data and to make a decision on whether any transient event is detected from the data. It also discusses the state estimation and V-Q algorithm of voltage stability for predicting the margin to instability. It also shows some interesting cases for which the stability margin has been calculated. Also it describes the QV modal analysis which is used to verify the test results obtained from the voltage stability algorithm.

The fourth section describes the conclusion drawn from this work.

2. VOLTAGE STABILITY ASSESSMENT AND STATE ESTIMATION USING SYNCHROPHASORS

2.1 VOLTAGE INSTABILITY DETECTION

Until recently it was difficult to predict and detect voltage instability because of the fact that this form of instability can manifest itself in various forms – as a purely steady state phenomenon, or a purely dynamic phenomenon, and sometime a hybrid. Advances in technology have made it possible to monitor and predict voltage instability. Although shunt capacitors help in increasing power transfers, the same power transfers tend to bring the operating voltage nearer the instability point. As such it is a challenge to monitor the present operating point and its proximity to the point of collapse using the traditional SCADA based system. Synchronized phasor measurement units are a relatively new technology which allows operators to accurately monitor the state of the system given enough points of measurement. Synchrophasors measure voltages and currents at different locations on the grid with an accurate time stamp on each reading. Since these measurements are synchronized with a common time reference such as GPS clock, it is possible to compare two quantities in time.

Reference [2] discusses voltage instability detection and mitigation in the Eskom power system in South Africa. Eskom used the traditional method of load-shedding to prevent voltage collapse - but the problem with the traditional scheme was that a large amount of load was needed to be shed by the time the problem was detected. So they developed a new real-time detection and mitigation algorithm using synchrophasors. The SVP collects data from field devices and computes the state of the system. The system

state and network data is then sent to the computer which calculates the voltage collapse indices given below:

1) The first index is the reactive power voltage margin (QVM) with respect to a bus i:

$$QVM = Q_{Maximum} - Q_{Operating} \tag{2.1}$$

where:

$Q_{Operating}$ is the measured reactive power at bus i; and

$Q_{Maximum}$ is the maximum reactive power threshold at bus i

The QVM indicates the minimum inductive load necessary to cause voltage collapse under steady state conditions.

2) The second index is the Incremental Reactive Power Cost (IRPC). It gives the reactive power required by the reactive power sources to feed each additional MVAr at bus_j. It is given below:

$$IRPC_j = \sum_{k=1}^{n} \frac{\Delta Q_{gen_K}}{\Delta Q_{bus_j}} \tag{2.2}$$

These stability indices helped Eskom in determining how close the system was to voltage collapse and to propose an effective load-shedding scheme before voltage collapse. The computed indices are then sent back to the SVP. If the indices show that an action is required immediately, the SVP issues load-shedding command to the known weak buses in the system using an automatic control. If the indices show that there might be a problem some time later, the SVP alarms the operator who may issue a load-shedding command through manual control. Thus the voltage stability indices reduce the unnecessary customer interruptions.

Reference [9] provides another algorithm of calculating real-time voltage stability index. It proposes a new online voltage stability index based on synchrophasors that computes the steady state voltage stability limit for the system. For prevention of voltage collapse, an effective online algorithm is required. Many utilities use dynamic simulations for assessing voltage stability - but the problem with dynamic simulations is that they are time consuming and therefore not suitable for online applications. Other methods based on state estimation also will not be effective in online environment since the SCADA-based state estimator take minutes to update the current state of the system. With utilities worldwide beginning to use synchrophasor measurements, it is possible to monitor and analyze the power system behavior. Synchrophasor data consists of values of parameters such as the bus voltage, frequency, bus angle etc with a precise time stamp. Because of the precise time stamp, it makes it possible to compare the quantities at a particular time instant. Three types of load margins are computed using synchrophasor data [9]. Based on these indices, the voltage stability index is calculated. Consider a simple 2 bus system show below in Figure 2.1. The active power *P* and reactive power *Q* at the load bus can be calculated using the equations given below:

$$P = \left[\left(V_s \cos\delta - V_r \right) \frac{R}{R^2 + X^2} + V_s \sin\delta \frac{X}{R^2 + X^2} \right] V_r \tag{2.3}$$

$$Q = \left[\left(V_s \cos\delta - V_r \right) \frac{X}{R^2 + X^2} - V_s \sin\delta \frac{R}{R^2 + X^2} \right] V_r \tag{2.4}$$

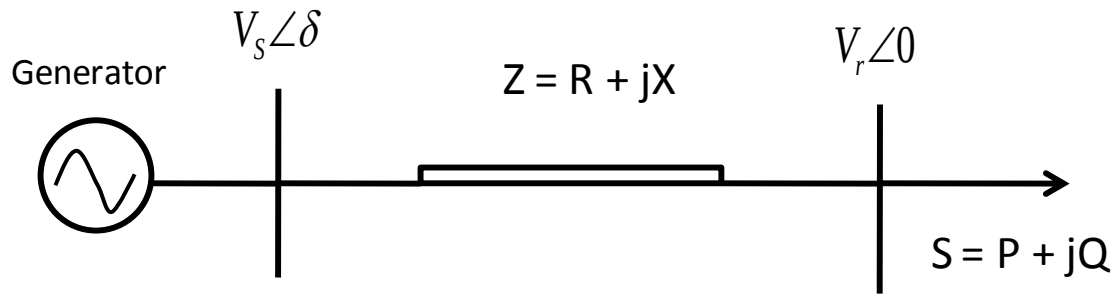

Figure 2.1 Simple 2-bus system to determine VSI

With the bus voltages and angles known from synchrophasor data, the active power *P* and the reactive power *Q* can be computed. Also the maximum real power P_{max} that can be transferred across the transmission line can be calculated using Eq. (2.5) below, assuming that the reactive power remains constant. Similarly, the maximum reactive power Q_{max} and maximum apparent power S_{max} can be computed using Eq. (2.6) and (2.7) respectively, assuming that the active power *P* and power factor angle remain constant respectively.

$$P_{\max} = \frac{QR}{X} - \frac{V_s^2 R}{2X^2} + \frac{|Z_L| V_s \sqrt{V_s^2 - 4QX}}{2X^2} \tag{2.5}$$

$$Q_{\max} = \frac{PX}{R} - \frac{V_s^2 X}{2R^2} + \frac{|Z_L| V_s \sqrt{V_s^2 - 4PR}}{2R^2} \tag{2.6}$$

$$S_{\max} = \frac{V_s^2 \left| Z_L - \left(\sin\theta X + \cos\theta R\right)\right|}{2\left(\cos\theta X - \sin\theta R\right)^2} \tag{2.7}$$

With the values of P_{max}, Q_{max}, S_{max}, three different load margins can be calculated as given by Eq. (2.8), (2.9) and (2.10). Based on these margins, the voltage stability index

can be computed by Eq. (2.11). A small value of VSI suggests that the bus of interest is closer to the instability point. At the point of instability, the value of VSI will be zero.

$$P_{margin} = P_{\max} - P \tag{2.8}$$

$$Q_{margin} = Q_{\max} - Q \tag{2.9}$$

$$S_{margin} = S_{\max} - S \tag{2.10}$$

$$VSI = \min\left(\frac{P_{margin}}{P_{\max}}, \frac{Q_{margin}}{Q_{\max}}, \frac{S_{marign}}{S_{\max}}\right) \tag{2.11}$$

In order to compute the VSI for large interconnected systems, the system is divided into three subsystems: the internal system, the boundary system and the external system. The internal system consists of three types of buses: load bus, tie bus and the source bus. The injection currents into the three buses are given below:

$$\begin{bmatrix} i_L \\ i_T \\ i_G \end{bmatrix} = \begin{bmatrix} Y_{LL} & Y_{LT} & Y_{LG} \\ Y_{TL} & Y_{TT} & Y_{TG} \\ Y_{GL} & Y_{GT} & Y_{GG} \end{bmatrix} \begin{bmatrix} v_L \\ v_T \\ v_G \end{bmatrix} \tag{2.12}$$

where the subscripts L,T, G stand for load bus, tie bus and source bus respectively. Thus the load bus voltage is given as:

$$v_L = Z_{LL} i_L + Z_{LT} i_T + H_{LG} v_G \tag{2.13}$$

where $Z_{LL} = (Y_{LL} - Y_{LT} Y_{TT}^{-1} Y_{TL})^{-1}$, $Z_{LT} = -Z_{LL} Y_{LT} Y_{TT}^{-1}$, $H_{LG} = Z_{LL}(Y_{LT} Y_{TT}^{-1} Y_{TG} - Y_{LG})$

With the load bus voltage, the equivalent voltage source for the j^{th} load bus and the line impedance Z_{equj} can be calculated as given below. With v_{equj} and Z_{equj}, the VSI for j^{th} load bus can be calculated using equations (2.5)-(2.11).

$$v_{equ_j} = \sum_{k=1}^{M} H_{LGjk} v_{GK} + \sum_{i=1, i\neq j}^{N} Z_{LLji} \left(\frac{-S_{Li}}{v_{Li}}\right)^* \tag{2.14}$$

$$Z_{equj} = Z_{LLjj} \tag{2.15}$$

The various other approaches used to determine the voltage stability of a system are described in references [10], [11], [12], [13]. Reference [10] describes a methodology based on mathematical expression for a simple two-bus radial system to find the voltage stability of a system. The method is simple, but for larger systems, reduction to a two-bus system becomes difficult. Voltage stability estimation based on local monitoring is discussed in reference [11]. It describes the development of two indices, namely, Voltage Stability Load Bus Index (VSLBI) and Reactive Power Reserve Index (RPRI). It also sheds light on the protection and control scheme for voltage collapse and calculates the voltage stability of a system for different load models. Reference [12] discusses in detail the development of a voltage stability index based on a similar approach to the Z-index for monitoring dynamic voltage stability using synchrophasor data. Reference [13] describes voltage stability monitoring in the KEPCO system in Korea based on the index developed in reference [12].

2.2 STATE ESTIMATION USING SYNCHROPHASORS

State estimation is one of the important functions in any control center. Based on the results of the state estimator, many decisions related to security and market are taken. Most of the state estimators available today are based on SCADA measurements of active and reactive power flows and voltage magnitudes from the field devices. Based on these measurements, the complete state vector consisting of positive sequence bus voltage magnitudes and angles is computed. The process of calculating the state vector is non-linear and iterative based on the least squares algorithm. But the problem with these state

estimators is that they are susceptible to convergence problems when the system is in a stressed condition. As a result, their reliability and accuracy is affected. PMUs are capable of improving the state estimator`s performance and also reducing the computation burden on the state estimator.

The traditional state estimation process is a non-linear iterative technique which requires a significant computational effort. Synchrophasors directly measure the state vector that is the bus voltage and bus angle. Thus if the PMUs are deployed at all buses, the state estimation process becomes direct and non-iterative [14]. The other advantage of synchrophasors is that since the measurements are available every few cycles, one can observe the dynamic behavior of the system. Another benefit is that redundancy is provided if branch currents are also measured. Reference [14] discusses the recent advances in state estimation using synchrophasors. It describes a state estimation algorithm based only on synchrophasors. It also provides a method of using synchrophasors with traditional measurements leading to a hybrid algorithm.

The state estimation algorithm based only on synchrophasors is shown in this section. The measurement set consists of positive sequence voltages and currents with normally distributed noise component having zero mean. The measurement vector is shown below:

$$M = \begin{bmatrix} V \\ I \end{bmatrix} + \begin{bmatrix} \varepsilon_V \\ \varepsilon_I \end{bmatrix} \tag{2.16}$$

where V and I are the true voltage and current measurements and ε_V and ε_I are the measurement error vectors respectively. The covariance matrix W of the measurement errors is shown below:

$$W = \begin{bmatrix} W_V & 0 \\ 0 & W_I \end{bmatrix} \tag{2.17}$$

If a π-representation is assumed for branches, the relationship between V and I could be shown as

$$I = \left| yA^T + y_S \right| V \tag{2.18}$$

where A is the current measurement-bus incidence matrix, y is a diagonal matrix of primitive series admittances of metered branches and y_s is the primitive matrix of all shunt admittances at the metered ends. Substituting equation (2.18) into (2.16) we get

$$M = \begin{bmatrix} I \\ yA^T + y_S \end{bmatrix} + \begin{bmatrix} \varepsilon_V \\ \varepsilon_I \end{bmatrix} \tag{2.19}$$

Equation (2.19) can be written as

$$M = B \cdot V + \varepsilon \tag{2.20}$$

The weighted least square estimates of the state vector V can be computed as shown

$$G.V = B^* \cdot W \cdot M \tag{2.21}$$

where G is the gain matrix as given below:

$$G = B^* \cdot W \cdot B \tag{2.22}$$

The state estimation process consists of finding the gain given in Eq. (2.22) for each measurement and then solving Eq. (2.21) for the state vector. Thus we see that the process is direct and non-iterative.

3. METHODOLOGY

3.1 SYNCHROPHASOR DATA

Synchronized phasor measurement data consists of analog and digital values of voltages and currents with an accurate time stamp. These quantities are collected from various locations in the power system, time-aligned and then processed as one single data set. The IEEE Standard C37.118-2005 has been developed for synchrophasor measurements. The standard defines the convention used for measuring the phasors, provides a methodology of determining the precision of measurements [15]. It also defines communication formats required for data transmission in real-time.

The basic concept of synchrophasor measurement is explained here. Synchrophasors provide a way of representing voltage and current phasors with respect to an absolute time reference. This time reference could be provided by high accuracy clocks synchronized to coordinated universal time such as a GPS clock. The phasor representation of a constant sinusoidal signal produced by a PMU is shown in Figure 3.1.a and Figure 3.1.b. The time tag denotes the reporting instant and is the reference for the sinusoidal signal. The phase angle of the phasor is calculated by finding the angular separation between the reporting time and the peak of the sinusoid. Thus we see that in Figure 3.1.a the peak of the sinusoid coincides with the reporting instant and thus the angle of the phasor is 0 deg. while in Figure 3.1.b the angle is -90 deg. since the sinusoid crosses zero at the timetag.

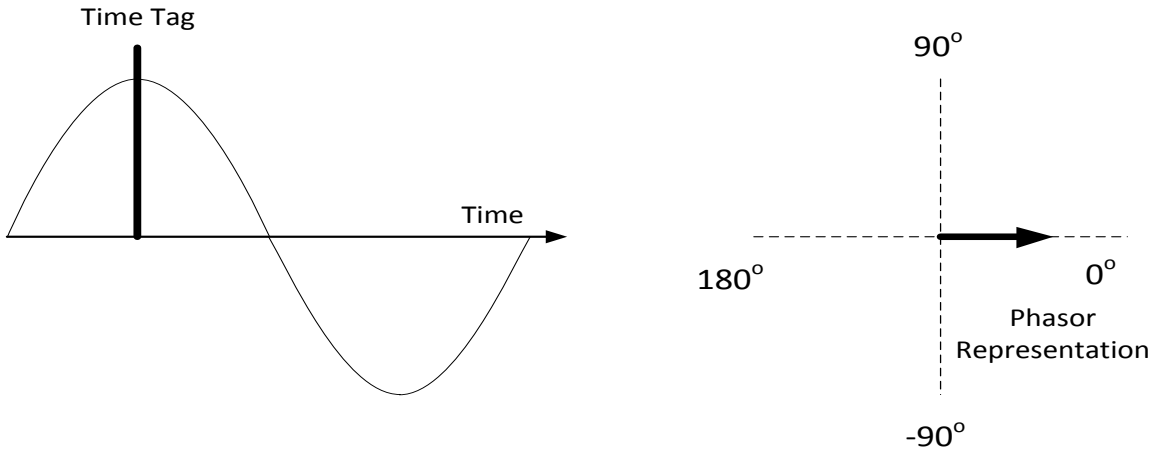

(a)

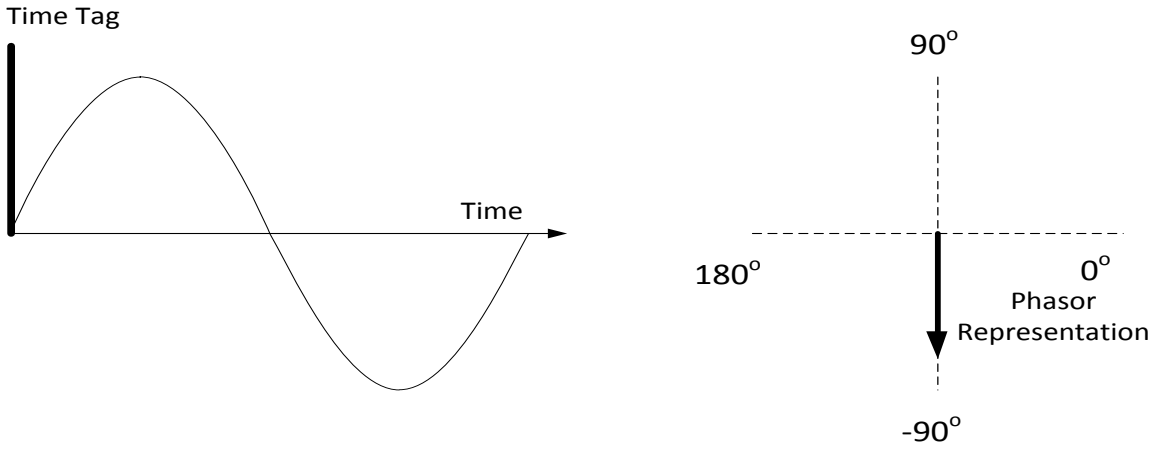

(b)

Figure 3.1.Synchrophasor representation and angle convention [2]

Reference [15] also throws light on the requirements for compliance with the standard. Thus compliance with IEEE Standard C37.118-2005 requires synchrophasor

measurements to meet the synchrophasor definition and conform to the communication protocol for reporting the measurements. Thus, as per the standard the phase angle convention is as shown in Figures 3.1.a and 3.1.b. Also the standard states that the reporting rates for PMU`s can be from 10 samples per second to 60 samples per second. It also mentions that the reporting times shall begin at the top of second. The standard also describes the accuracy of measurement and the different communication protocols to be used for reporting the readings.

Reference [16] describes the development of a specific synchrophasor network and applications such as modal analysis of angle differences between measurement locations. It gives the physical overview of where the PMUs are installed in Texas and also describes the equipment details, device settings and network problems and solutions. The SVP and a computer for display and processing are installed in a laboratory at UT Austin. The SVP acts as the central data collection center and gathers and time-aligns the PMU data from all locations and provides the coherent data set to IEEE C37.118 clients. The data archival software allows doing post-disturbance analysis. Figure 3.2 shows the variation of the average of the angle of McDonald bus with respect to UT Austin bus for one hour. We observe that the angle varies from an initial value of -12.25 deg. to -26.02 deg. at the end of one hour. Such a variation indicates the high penetration of wind energy in West Texas which is the main reason for this variation. So performing modal analysis of the angles obtained from synchrophasors helps in identifying the modes and the corresponding damping factor due to wind penetration. Also the frequency data from the PMUs help in identifying any generator tripping.

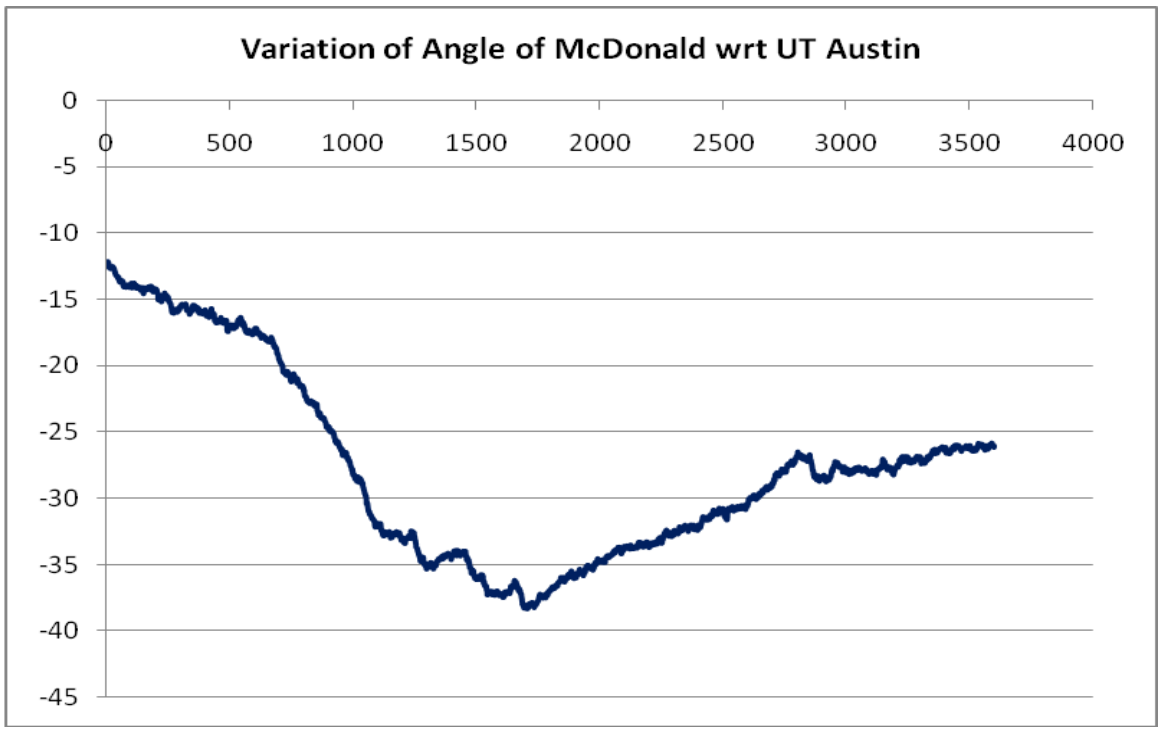

Figure 3.2 Variation of angle of McDonald with respect to UT Austin

3.2 V-Q CURVES FOR VOLTAGE STABILITY ANALYSIS

P-V and V-Q curve methods have been used for many years to study the voltage stability phenomena. These methods are generally offline methods which are used for both planning and operational studies. The V-Q curve method was developed to eliminate the problems encountered in convergence of power flow program of stressed cases close to the maximum power transfer point [17]. The convergence problem was eliminated by fixing the voltage at the critical bus. The V-Q curve describes the relationship between the reactive power injection Q_c at a given bus and the voltage at that bus [18]. This relationship can be determined by connecting a fictitious generator with zero active

power and recording the reactive power Q_c generated by it for a series of voltage schedules at that bus.

Reference [17] explains in detail the V-Q curve methodology. A flowchart for the V-Q method is shown in Appendix F. For the base case or any other case such as an outage, multiple power flows are run for a series of voltage magnitudes scheduled at the critical bus. The selected bus is converted to a PV bus by connecting a fictitious synchronous condenser or a synchronous generator with zero active power. For each voltage schedule the reactive power of the fictitious generator is noted and the V-Q curve is produced by plotting the reactive power injection against the voltage. The operating point is at zero reactive power of the fictitious generator if there is no shunt compensation available at that bus. If shunt compensation is provided at the bus, then we plot the characteristics of the shunt reactive compensation on the V-Q curve and the operating point is the intersection of the V-Q curve characteristics and the compensation characteristics. The advantages of V-Q curve method are [17]:

1) Convergence is not an issue even on the unstable part of the curve.
2) The method is fast and it converges in very few iterations.
3) Since voltage stability is closely related to reactive power, one can compute the reactive power margin at the test bus from the V-Q curve and thus this margin can be used as reliability index. The reactive power margin is the MVAr distance between the operating point and the bottom of the curve and is shown in Figure 3.2.
4) Reactive power outputs of generators and SVC`s can be plotted on the V-Q curve. At the bottom of the curve, the generators providing reactive power are operating at their

limits. Thus the generator reactive power and reactive power reserve at the operating point can be found.

5) Indication regarding voltage "stiffness" is provided by the slope of the V-Q curve.

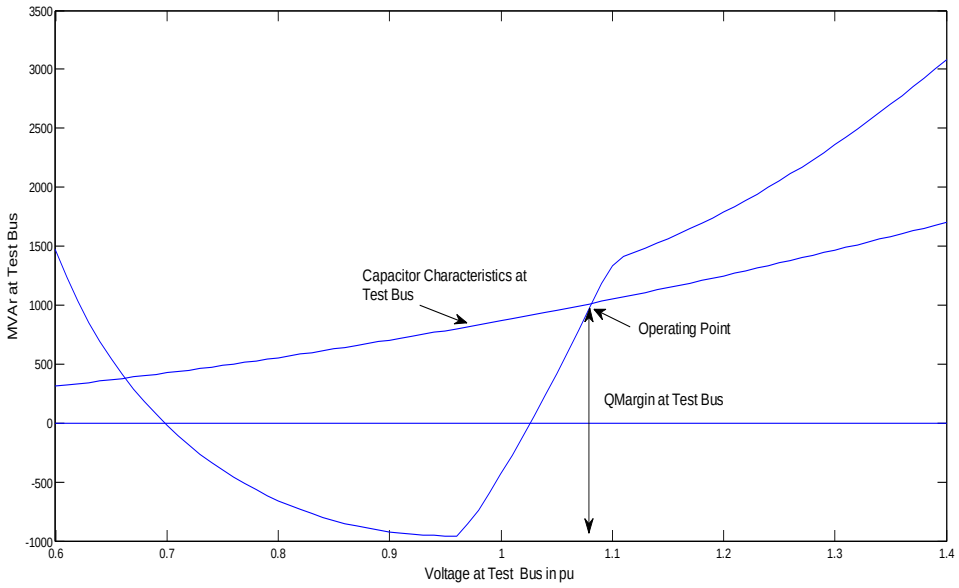

Figure 3.3 V-Q curve and reactive power margin

The disadvantages of the V-Q curve methodology are given below [17]:

1) The method is artificial and provides local area evaluation.
2) One needs to develop V-Q curves for many buses in the system and for every contingency and every power level to assess the voltage stability of the system.
3) Another disadvantage is that, for a given operating point, V-Q curves give an idea of local compensation required rather than global optimal compensation.

3.3 PROPOSED METHODOLOGY FOR VOLTAGE STABILITY ASSESSMENT

The proposed algorithm for voltage stability estimation is shown in Figure 3.4. The first step of the algorithm is to get the voltage and current synchrophasor data. The next step is to check for bad data in the samples. Then we find the standard deviation of the voltage magnitudes and angles. The next step is to check if the standard deviation of voltage magnitudes is within the prescribed limits. If it is not within limit, then we find dv/dt and $d\theta/dt$ for all the samples. We check if dv/dt or $d\theta/dt$ are within limits, if they are outside the limits, we get out of the loop and wait for the next data sample. It also indicates that there is some transient event occurring. If the standard deviation of voltage magnitude is within limits, we then check if standard deviation of voltage angles is within limits. If not within limits, we find $d\theta/dt$ for all samples. We again check if $d\theta/dt$ is within limits, if it is then we get out of the loop and wait for the next data sample. It again indicates the presence of a transient event in the data. If the standard deviation of both voltage magnitudes and angles is within limits, we then check the difference of average of voltage magnitudes or voltage angles of present iteration and previous iteration. If either of the difference is not within limits, we do the state estimation to find the present operating point and the reactive powers of generators. After state estimation, we find the reactive power margin using the VQ analysis algorithm.

3.3.1 Test System. The voltage stability algorithm was tested on the CIGRE 10-bus system shown in Figure 3.5. The steady state system data for a particular operating condition is given in Appendix A. Reference [1] describes in detail the steady state simulation for base case conditions of power flow. GEN1 and GEN2 are two remote generators separated from load area by 5 parallel 500-KV transmission lines.

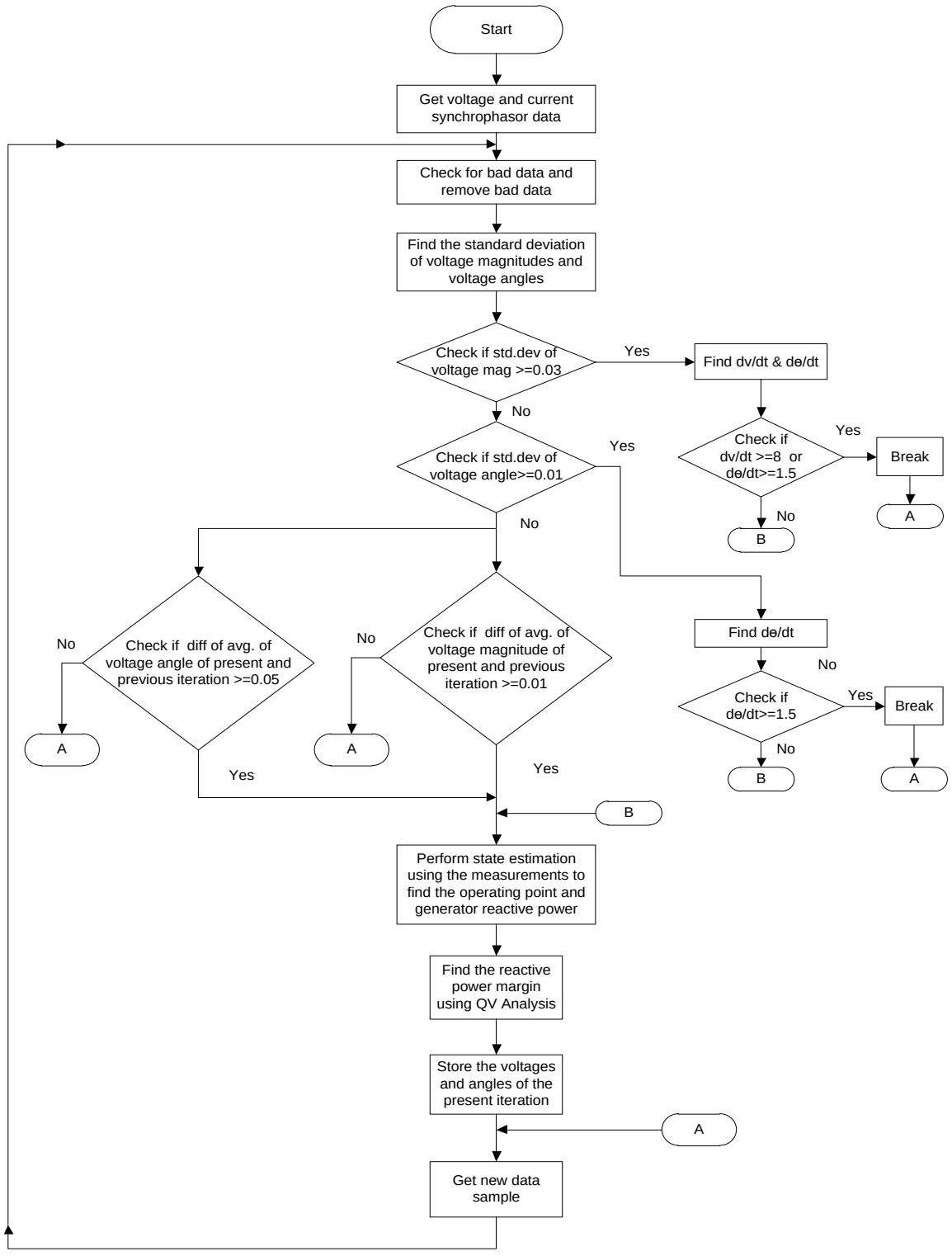

Figure 3.4 Algorithm for voltage stability estimation

The load area has one generator and two large loads. The load at INDUST bus is an industrial load consisting of large induction motors. Thus it is modeled as constant power load. The load at LOAD bus comprises of both residential and commercial load. Half of the load is constant power load and the other half is resistive. The load area is compensated by three shunt capacitor banks. The power flow results for base case are shown in Figure 3.6. The base case loads are: Bus INDUST – Active Power=3000 MW, Reactive Power=1800 MVAr; Bus LOAD – Active Power=3000 MW, Reactive Power=0.

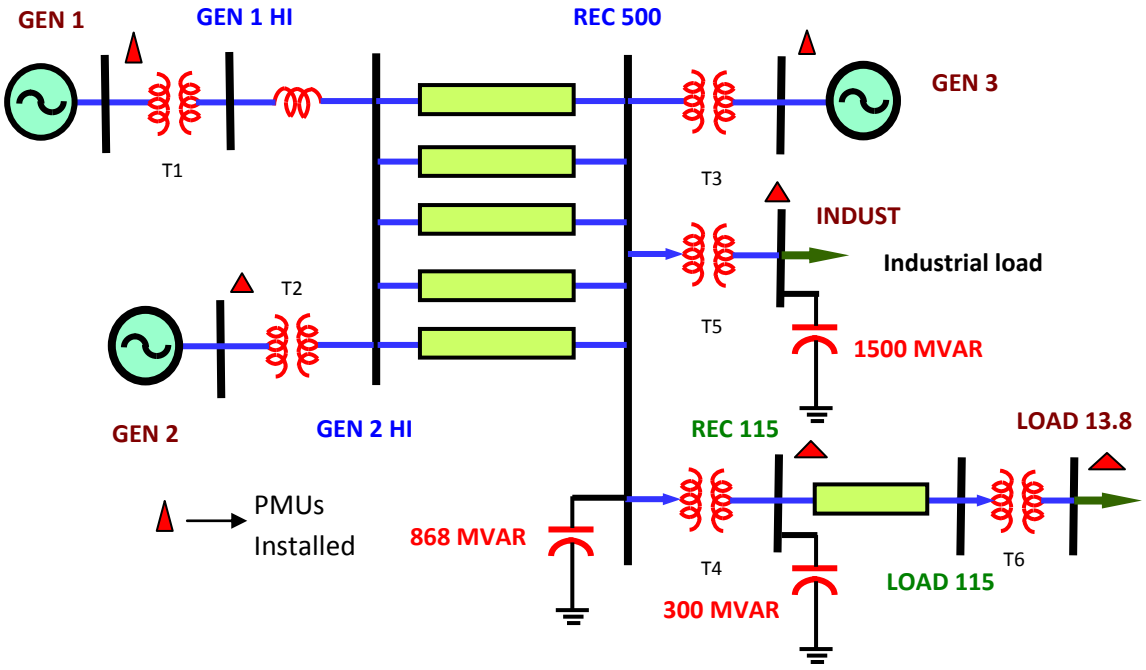

Figure 3.5 10-Bus CIGRE test system

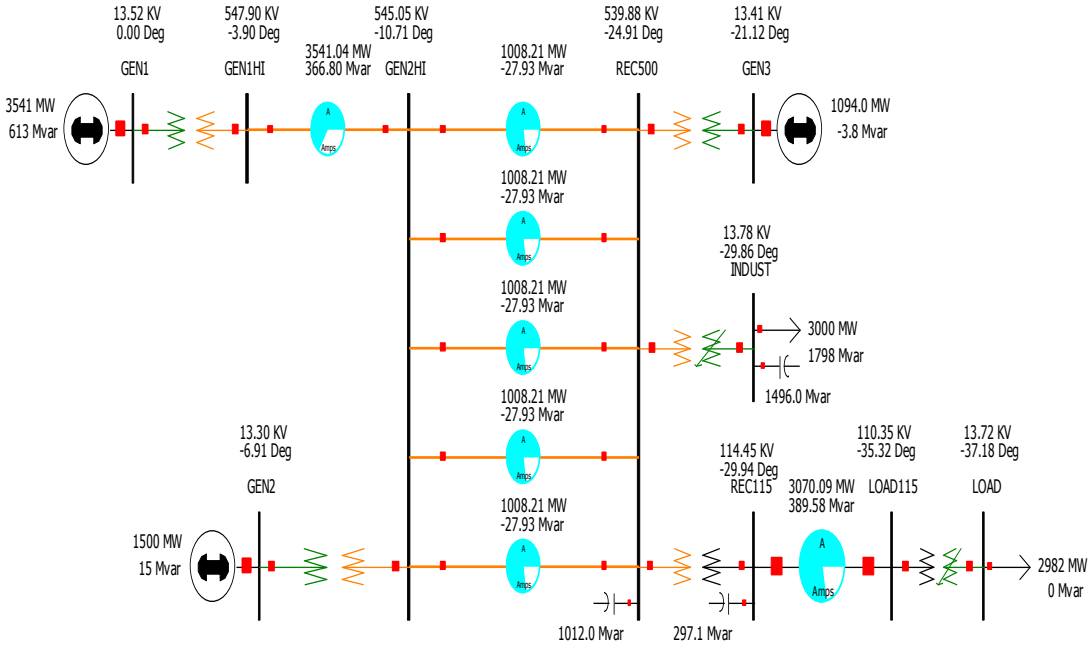

Figure 3.6 Power flow results for base case

3.3.2 Obtaining The Test Synchrophasor Data. The synchrophasor data for the 10-bus system was obtained by running transient stability analysis in PowerWorld [19]. The dynamic data for the generator, excitation system and governor is based on Unit F18 in Appendix D of reference [20] and is shown in Appendix B. The transient stability tool in PowerWorld was run for various cases such as line outage, load increase and capacitor bank outage. For every case, the bus voltages, bus angles, load currents and angles at the various measurement points were recorded at every quarter cycle. Thus the data from transient analysis tool represents the data that would be expected from various PMUs installed in the system, with each PMU having a reporting rate of 30 samples per second. It is assumed that the PMUs have been installed at: GEN1, GEN2, GEN3, REC115,

INDUST and LOAD buses as shown by the triangle symbol in Figure 3.5. Thus we have voltage and current phasor data streaming in from these buses at the typical synchrophasor measurement rate. This data first goes through the bad data screening check and then processed as mentioned in the algorithm presented earlier. The algorithm first checks for the presence of any transient event in the data by checking whether the standard deviation of voltage magnitudes or voltage angles is within limits. If this condition is satisfied then it checks the difference between the average values of voltage magnitude or voltage angles of present and previous iteration. Based on these checks the algorithm decides whether the system state has changed and correspondingly takes the decision of whether or not to process the data further and perform a state estimation leading to the computation of reactive power margins from V-Q analysis. A sample synchrophasor data obtained from simulations is shown in Table 3.1. The bus voltage magnitudes and angles of generator buses are shown. The voltage magnitudes of generator buses and the generator reactive power output are shown in Figures 3.7 and 3.8 respectively. The plots shown in Figures 3.7 and 3.8 are drawn using the synchrophasor data recorded for line outage between buses GEN2HI and REC500. The line outage event is simulated 200 seconds and the line is taken out at t=10 secs. We can see a brief reduction in voltage magnitude plot at 10 secs because of one line being taken out.

3.3.3 State Estimation With The Test Synchrophasor Data. The voltage magnitudes, voltage angles, current magnitudes and current angles from the synchrophasor data are then used to perform a state estimation. State estimation is done to compute the present operating point of loads and also to find the reactive power output of generators. The latter is monitored to check if the generators hit their corresponding

Table 3.1 Sample of synchrophasor data

Bus GEN1 Voltage (pu)	Bus GEN2 Voltage (pu)	Bus GEN3 Voltage (pu)	Bus GEN1 Angle (Degrees)	Bus GEN2 Angle (Degrees)	Bus GEN3 Angle (Degrees)
0.9582	0.9410	0.9614	-0.0056	-6.9119	-21.1130
0.9807	0.9661	1.0056	-0.0031	-6.9088	-21.1250
0.9911	0.9784	0.9545	-0.0057	-6.9065	-21.1117
1.0020	1.0157	0.9623	-0.0103	-6.9076	-21.1255
1.0109	0.9507	0.9578	-0.0091	-6.9009	-21.1119
0.9817	0.9677	0.9485	-0.0021	-6.9059	-21.1157
0.9502	0.9624	0.9682	-0.0170	-6.8889	-21.1241
0.9652	0.9253	0.9665	0.0061	-6.9039	-21.1307
0.9588	0.9552	1.0026	-0.0012	-6.8890	-21.1324
1.0270	0.9281	0.9670	0.0070	-6.9142	-21.1247
0.9677	0.9808	0.9507	0.0027	-6.9017	-21.1264
0.9950	0.9462	1.0041	0.0049	-6.9096	-21.1261
0.9762	0.9660	0.9967	-0.0148	-6.9010	-21.1122
0.9978	0.9531	0.9674	-0.0102	-6.9011	-21.1250
0.9647	0.9701	0.9419	-0.0045	-6.9289	-21.1106
0.9520	0.9520	0.9631	0.0011	-6.9203	-21.1273
0.9516	0.9738	0.9689	0.0113	-6.9214	-21.1123
0.9898	0.9788	0.9775	-0.0029	-6.9030	-21.1272
0.9765	0.9982	0.9668	0.0126	-6.8923	-21.1202
0.9761	0.9601	0.9809	0.0048	-6.9103	-21.1123
1.0084	0.9212	0.9798	0.0117	-6.8989	-21.1261
0.9858	0.9472	0.9470	0.0013	-6.9015	-21.1264
0.9840	0.9911	0.9530	-0.0066	-6.9175	-21.1020
1.0118	0.9426	0.9572	-0.0148	-6.9030	-21.1125
0.9639	0.9832	0.9618	0.0016	-6.9145	-21.1263
0.9939	0.9665	0.9656	0.0082	-6.8918	-21.1155
0.9967	0.9927	0.9722	-0.0029	-6.9073	-21.1256
0.9751	0.9248	0.9114	-0.0054	-6.8906	-21.1149
0.9843	0.9600	0.9629	-0.0031	-6.9113	-21.1078
0.9567	0.9398	0.9968	-0.0110	-6.9011	-21.1380

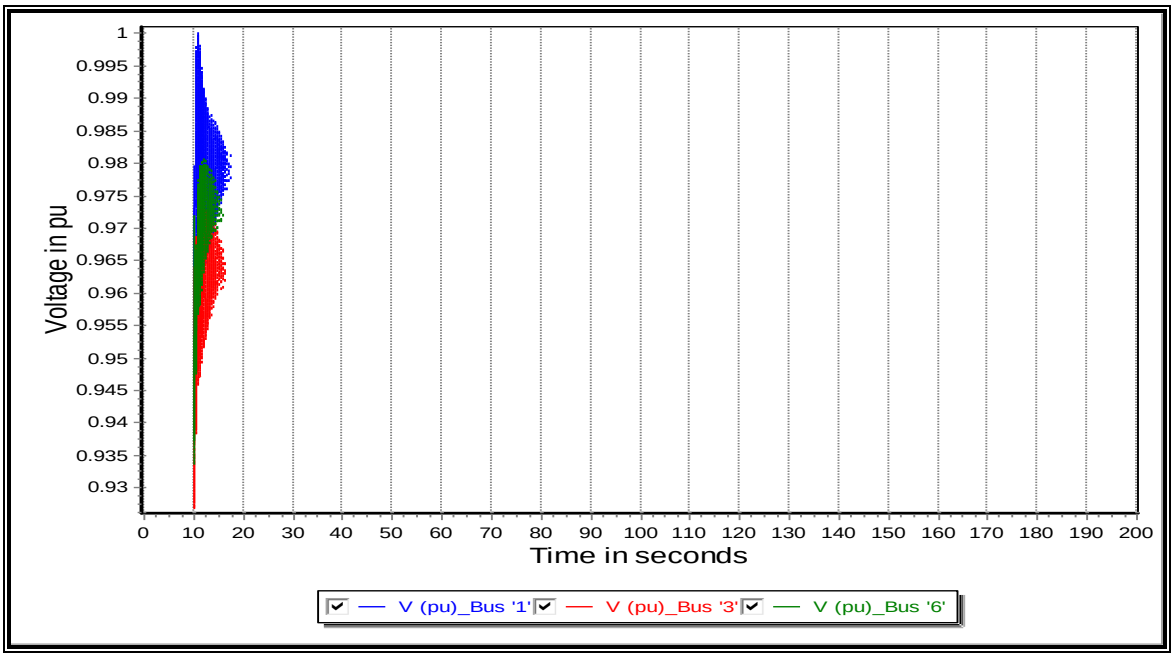

Figure 3.7 Voltage magnitudes of generator buses

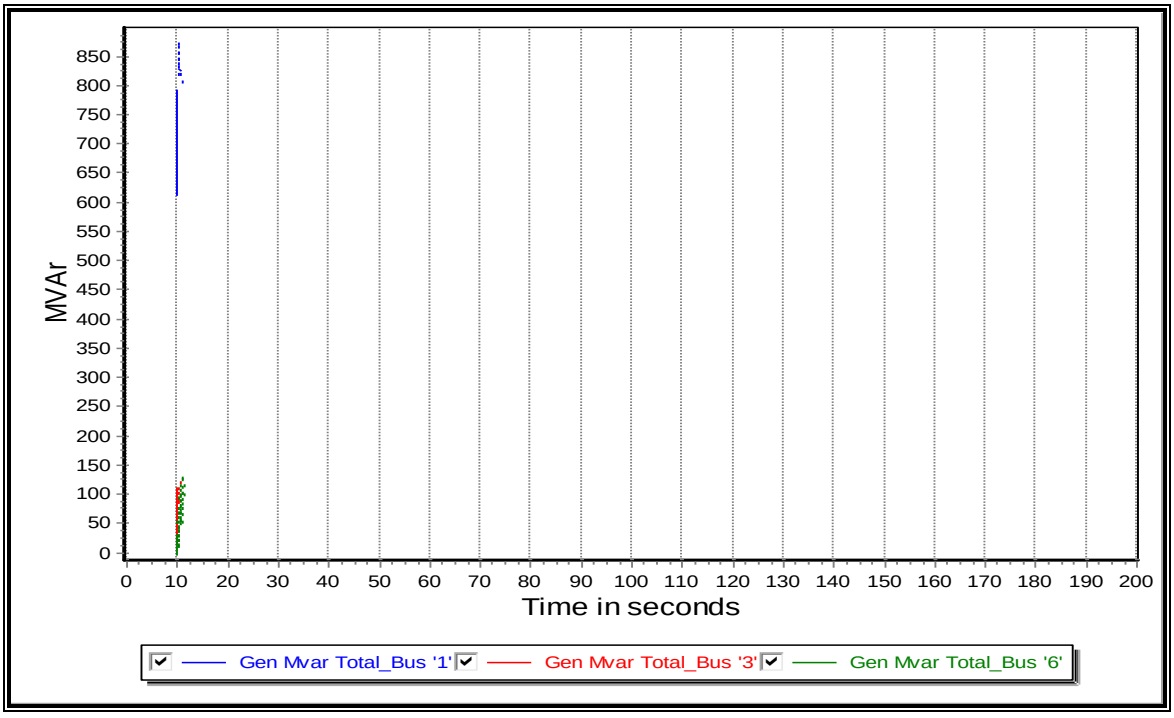

Figure 3.8 Reactive power output of generators

reactive power limits, which is generally considered as a sign of the system approaching the point of instability. In state estimation we assign a value to an unknown state variable based on measurements from the system according to a statistical criterion [21]. The most common statistical criterion used in state estimation is the sum of the squares of the differences between the estimated and the true value of the function. In a power system, the state variables are the bus voltages and angles. The inputs to the state estimator are the power measurements such as bus voltage magnitude, bus angles and power flows with random noise embedded in the measurements. The objective of the estimator is to produce a best estimate of the state variables. The active and reactive power measurements are non-linear functions of bus voltage magnitudes and angles. As such, the process of estimating the system states is non-linear and iterative. For the proposed voltage stability algorithm, the traditional state estimation method is used. Bus voltage magnitudes and angles and active and reactive power flows of the lines are used as the inputs to the state estimator. The freely available software Matpower [22] was used for the purpose of performing state estimation. As discussed in section 2.2, if there are PMUs installed on all buses in the system, then the complete state of the system is known and the estimation process becomes linear and simple - but this is a highly optimistic assumption since most of the utilities would install only a handful of PMUs and that too in several stages. Keeping this in mind, it is assumed that only a few buses in the system have PMUs installed. As a result, to make the system observable one needs active and reactive power flows on the lines as inputs to the state estimator. The active and reactive power flows are calculated using the voltage and current phasors from the PMU by using a pseudo power flow measurement technique. Reference [23] describes the pseudo power

flow measurement technique using the voltage and current phasors from PMUs. It is assumed that a PMU is connected at bus *i*, so using the voltage phasor of bus *i* and current phasor flowing from bus *i* to bus *j*, the pseudo active and reactive power flows from bus *i* to *j* can be calculated as shown in Eq. (3.1) and (3.2).

$$P_{ij_{pseudo}} = V_i I_{ij} \cos(\theta_i - \theta_{ij}) \tag{3.1}$$

$$Q_{ij_{pseudo}} = V_i I_{ij} \sin(\theta_i - \theta_{ij}) \tag{3.2}$$

The pseudo power flow measurements are similar to conventional power flow measurements and thus we do not need to modify anything in the state estimator. Any real world measurement is subject to noise due to A/D conversion, noise of communication channels etc. Thus to create noisy measurements, we added random Gaussian noise to the noise free measurements obtained from Power World as shown in Eq. (3.3)-(3.6) [23].

$$P - Q_{pseudo} = P - Q_{pseudo_{exact}} + unc_{flow} \cdot GN(0,1) \tag{3.3}$$

$$V = V_{exact} + unc_V \cdot GN(0,1) \tag{3.4}$$

$$I = I_{exact} + unc_I \cdot GN(0,1) \tag{3.5}$$

$$\theta = \theta_{exact} + unc_\theta \cdot GN(0,1) \tag{3.6}$$

where, *unc* is the maximum uncertainty for each measurement type and

GN(0,1) is the additive Gaussian noise with zero mean and standard deviation 1.

The maximum measurement uncertainties for the measurements are given in Table 3.2.

Table 3.2 Maximum measurement uncertainties

Voltage Magnitude (pu)	Current Magnitude (pu)	Phase Angle (Degrees)
0.02	0.03	0.01

The standard uncertainties for the pseudo measurements are calculated by combining the standard uncertainties of the voltages and currents, which are used in computing the pseudo power flows. The standard uncertainties for the pseudo active and reactive power flows are given in Eq. (3.7) and (3.8) [23].

$$u(P_{ij_{pseudo}}) = \sqrt{\sum_{k=1}^{4} [\partial P_{ij_{pseudo}} / \partial p(k)]^2 \cdot [u(p(k))]^2} \tag{3.7}$$

$$u(Q_{ij_{pseudo}}) = \sqrt{\sum_{k=1}^{4} [\partial Q_{ij_{pseudo}} / \partial p(k)]^2 \cdot [u(p(k))]^2} \tag{3.8}$$

where,

$$p(k) = [V_i, \theta_i, I_{ij}, \theta_{ij}]$$

u(p(k)) is a vector containing the standard uncertainties of the measurement *p(k)*. The results of state estimation for the base case are shown in Table 3.3. The reactive powers of generators computed from state estimation are given in rows 12, 13 and 15 of Table 3.3. The results indicate that estimated values are very similar to those obtained from the power flow results shown in Figure 3.6.

3.3.4 Obtaining Voltage Stability Margins. The next step after state estimation is computing the reactive power margin at a representative bus in the load area, namely bus REC500. The state estimation gives the reactive powers of the generators and also active

Table 3.3 State estimation results (100 MVA base)

Measurement Type	Bus Name	Measurement (pu)	Estimation (pu)	Error
PF	1	35.4427	35.4427	0
PF	3	14.9559	14.9559	0
PF	8	30.7647	30.7691	1.94E-05
PT	6	-29.9793	-29.9789	1.6E-07
PT	9	-29.7533	-29.7546	1.69E-06
Va	3	-0.1205	-0.1205	0
Va	8	-0.5226	-0.5237	1.21E-06
Va	6	-0.3686	-0.3686	0
Va	7	-0.5211	-0.5212	1E-08
Va	10	-0.6488	-0.6477	1.21E-06
QF	1	6.1322	6.1322	0
QF	3	0.1556	0.1556	0
QF	8	3.9023	3.9019	1.6E-07
QT	5	-0.0375	-0.0380	2.5E-07
QT	6	-3.0249	-3.0236	1.69E-06
Vm	1	0.9811	0.9797	1.96E-06
Vm	3	0.9613	0.9613	0
Vm	8	0.9969	0.9960	8.1E-07
Vm	6	0.9673	0.9706	1.09E-05
Vm	7	0.9985	0.9955	9E-06
Vm	10	0.9917	0.9916	1E-08
Legend: PF - Active power flow from "From Bus"				
PT - Active power flow from "To Bus"				
QF - Reactive power flow from "From Bus"				
QT - Reactive power flow from "To Bus"				
Va - Bus voltage angle				
Vm - Bus voltage magnitude				

and reactive powers of loads. Thus, we can find out the most recently updated values of load demands. The active and reactive powers of loads obtained from state estimation are then used in the V-Q analysis. Every time the system state changes, we need to update the load operating point in the V-Q analysis. This is done by updating the bus matrix which

is used as an input for solving the power flow. As mentioned earlier in section 3.2, we do a series of power flows for different voltage schedules and note down the reactive power output of the fictitious synchronous generator placed at the test bus for V-Q analysis. For this system, the test bus is REC500. So a fictitious generator having zero active power output and infinite reactive power capability is connected at bus REC500. Also since there is shunt compensation already available at REC500, we plot the capacitor characteristics separately on the V-Q curve. The intersection of the capacitor characteristics and the V-Q curve is the present operating point of the system. The reactive power margin is calculated as the difference between the bottom of the V-Q curve and the operating point of the system.

3.4 TEST RESULTS

The proposed voltage stability algorithm was tested on the 10-bus system. The algorithm was tested for various scenarios such as the base load case, REC500 capacitor bank outage, line outage between buses GEN2HI and REC500 and load increase by 750 MW. For each of these cases, the synchrophasor data was produced by running transient analysis tool in PowerWorld. The data was then put through the algorithm to compute the V-Q curve and to find the reactive power margin.

Figure 3.9 shows the V-Q curve for the base case load. From the V-Q curve of Figure 3.9 we observe that the available reactive power margin at bus REC500 before voltage collapse is 1994 MVAr. Thus if the reactive power at bus INDUST increases by 1400 MVAr from the base case power, then the voltage at REC500 collapses and the system can no longer support the increased load demand. This has been verified by V-Q

modal analysis methodology explained in the next section. Since the bus at which we increase the load is different from the bus for which V-Q curve is plotted, we see that the actual reactive power increase is 1400 MVAr which is different from the reactive power margin we obtain from the V-Q curve, which is 1994 MVAr. This is because of the reactive power losses in the transformer connected between buses REC500 and INDUST.

Figure 3.10 shows the V-Q curve for REC500 capacitor bank outage. We observe that the reactive power margin drastically reduces from the base case as the shunt compensation at bus REC500 is removed. Also we see that the reactive power output of generators 1, 2 and 3 have increased by 88.19 MVAr, 103.12 MVAr and 197.64 MVAr respectively from the base case. Thus we see that the system is moving closer to instability point.

The third case presented is similar to the second case mentioned above but here the reactive power limits of the generators have been reduced and is shown in Figure 3.11. Sometimes it happens that the generators cannot provide the rated reactive power due to heating problems in the field winding and as such they operate with reduced reactive power capability. As a result, the reactive power margin at REC500 reduces further to 526.85 MVAr and the point of instability creeps closer to the operating point.

Figure 3.12 shows the V-Q curve for the line outage case. The load for this case is the same as the base case load. We again see the reduction in reactive power margin from the base case by 567 MVAr.

Figures 3.13 and 3.14 show the V-Q curve for the load increase case, without and with reduced reactive power capability of the generators respectively. The load is increased at LOAD bus by 750 MW. We observe from Figure 3.13 that the reactive

power margin is 1288 MVAr while it reduces to 817.58 MVAr when the generators are operated with reduced reactive power capability, as shown in Figure 3.14. The last case presented here is the worst case scenario that can take place where we have a line outage between buses GEN2HI and REC500, we have a REC500 capacitor bank outage and there is load increase at LOAD bus by 200 MW. The V-Q curve for this case is shown in Figure 3.15. We see that the system has a very small reactive power margin before the system collapses. The reactive power margin in this case is 258.11 MVAr. In all the V-Q curves, we see that the shape of the curve changes at two points – first, when the voltage at REC500 is 0.96 pu and second when the voltage at REC500 is 1.1 pu. The reason for the inflexion when REC500 voltage is 0.96 pu is that generators 2 and 3 hit their maximum reactive power limits. For the second point where REC500 voltage is 1.1 pu, the reason for change in the shape of the curve is that generators 2 and 3 hit their minimum reactive power limits. The summary of all the cases is shown in Table 3.4.

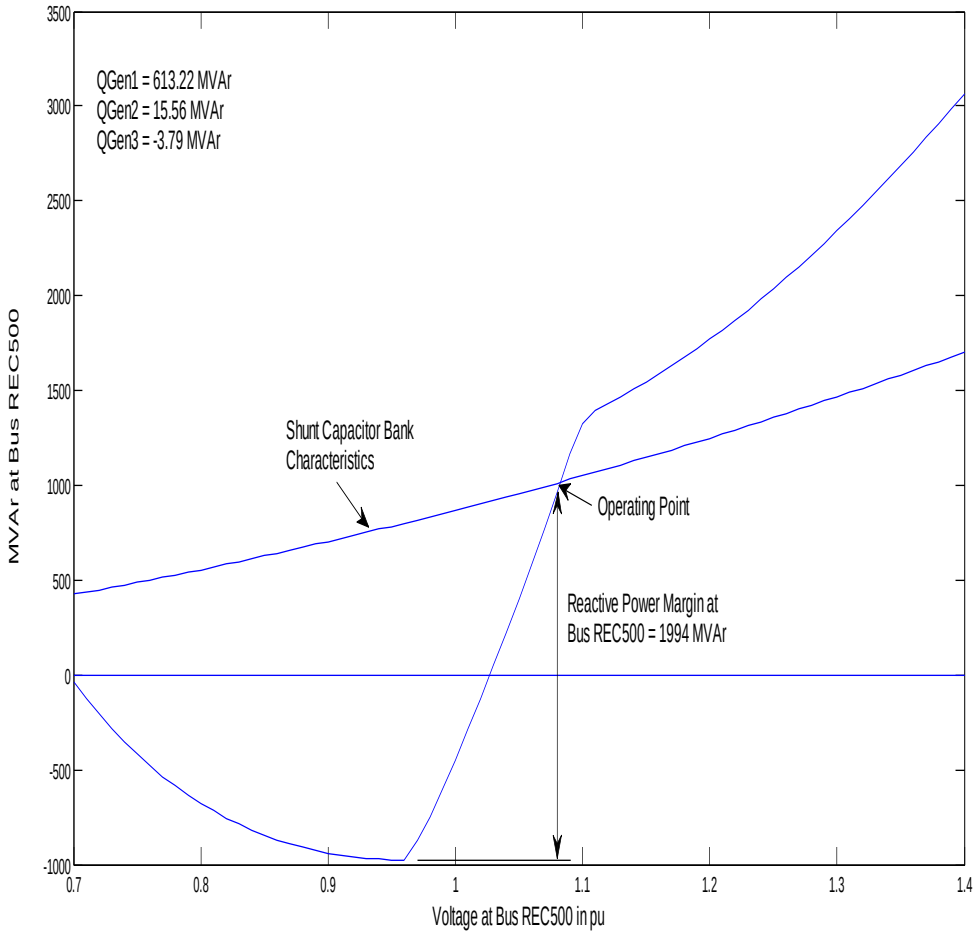

Figure 3.9 V-Q curve for base case load

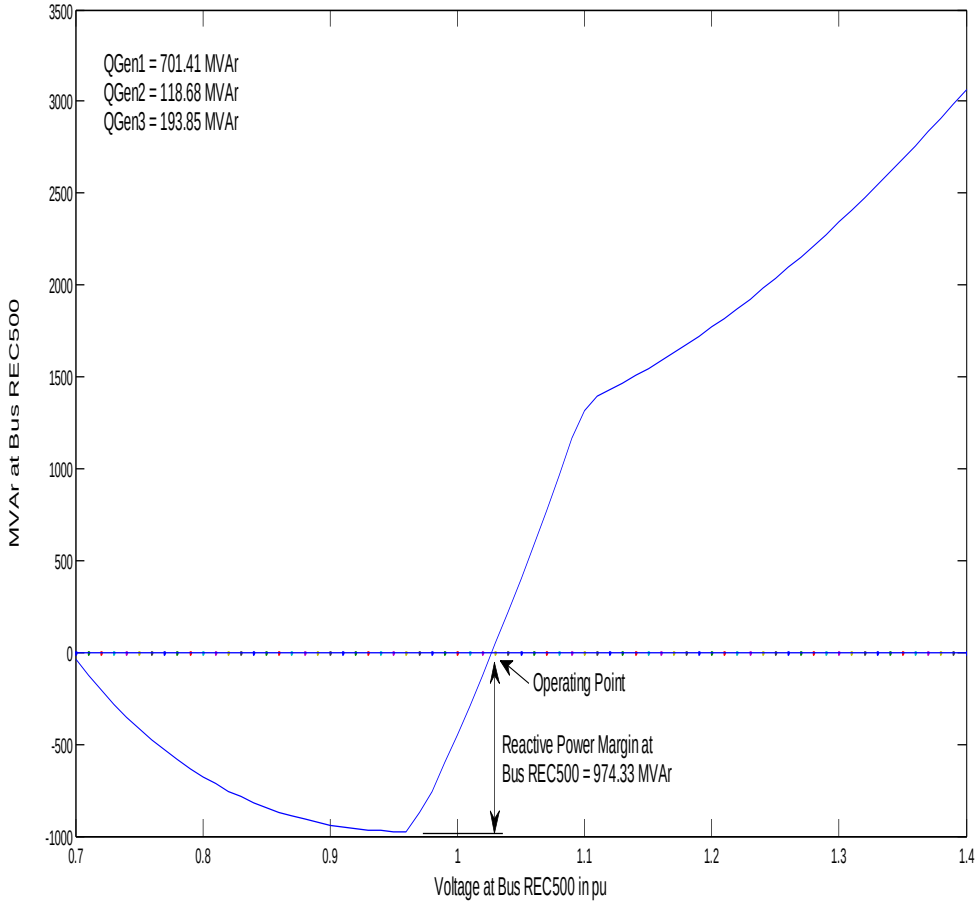

Figure 3.10 V-Q curve for REC500 capacitor bank outage

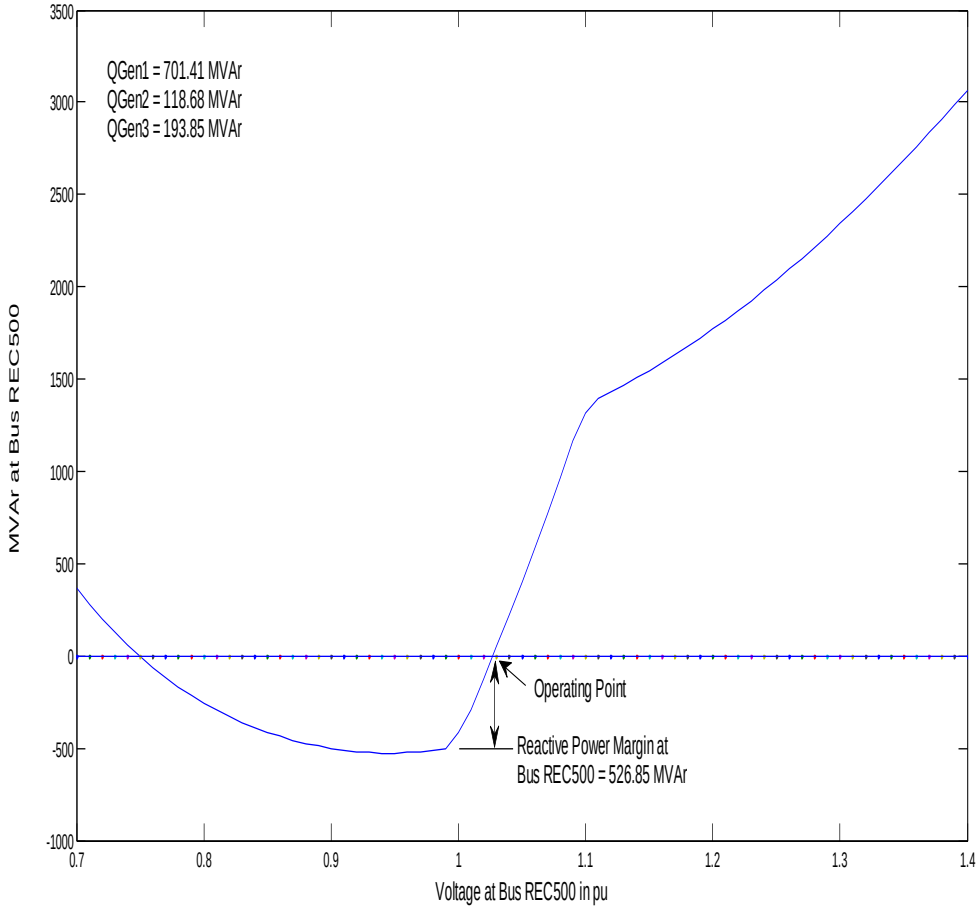

Figure 3.11 V-Q curve for REC500 capacitor bank outage with reduced Q_{limits} of generators

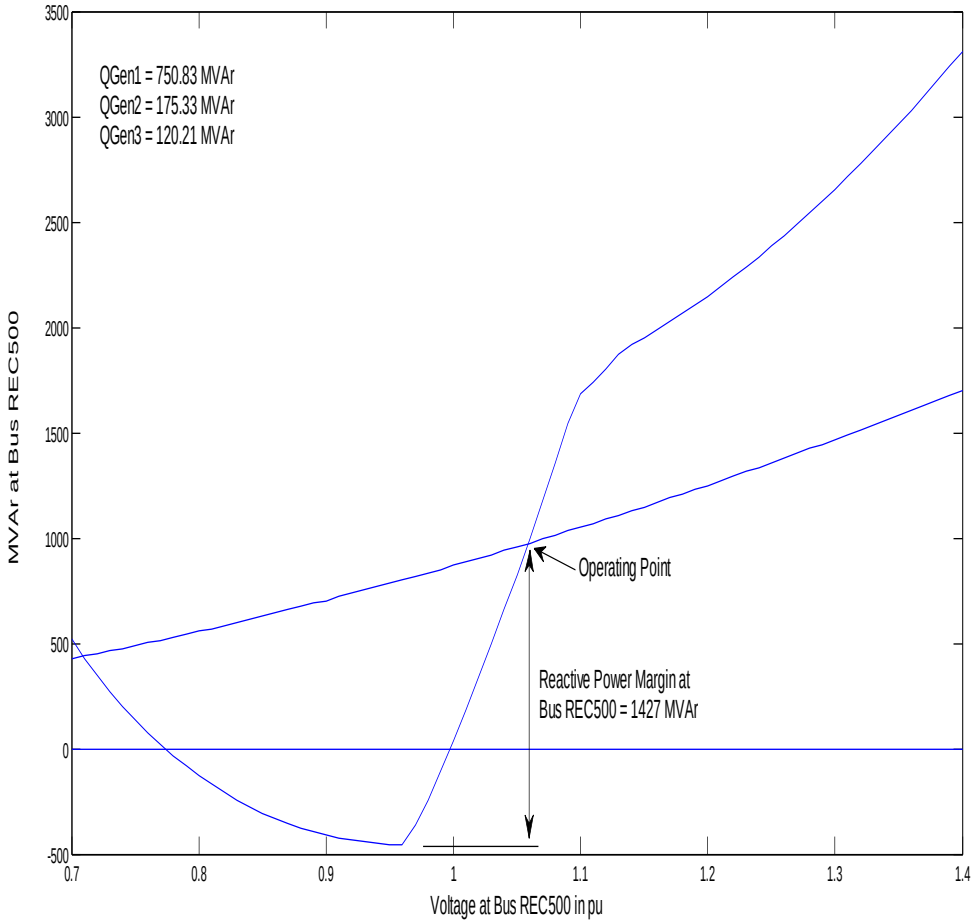

Figure 3.12 V-Q curve for line outage case

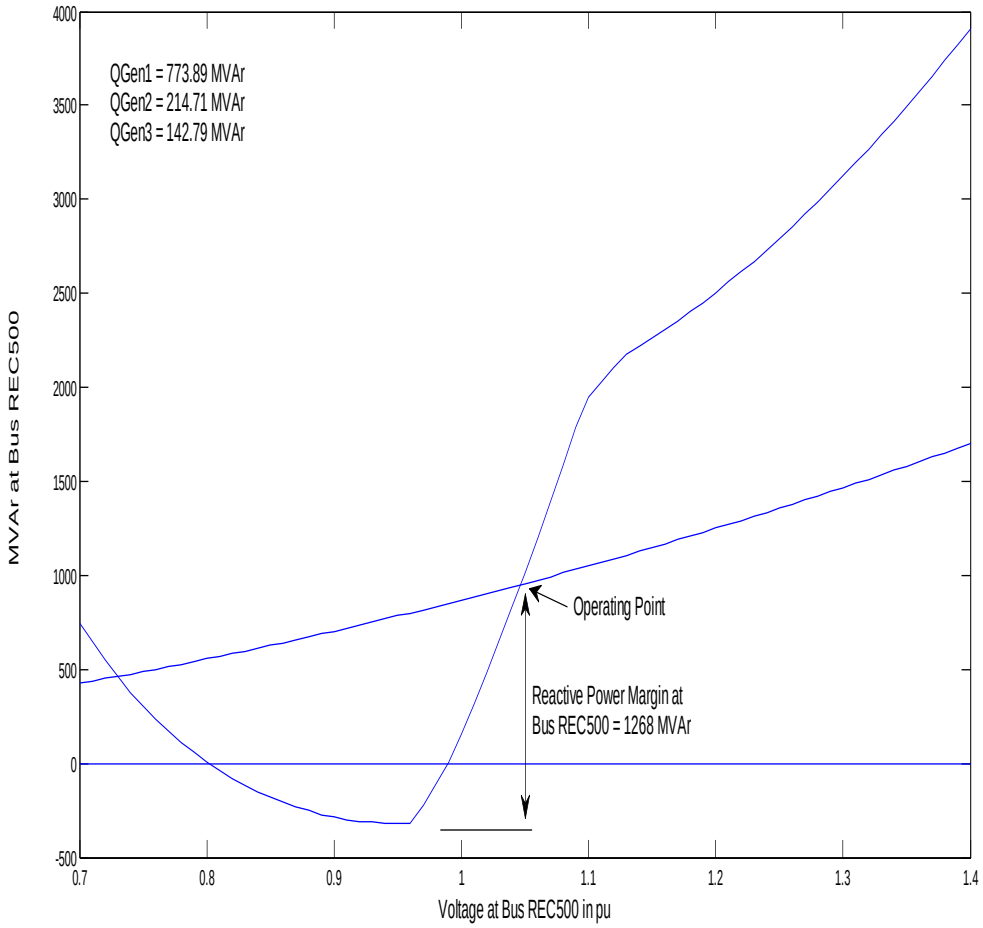

Figure 3.13 V-Q curve for load increase by 750 MW

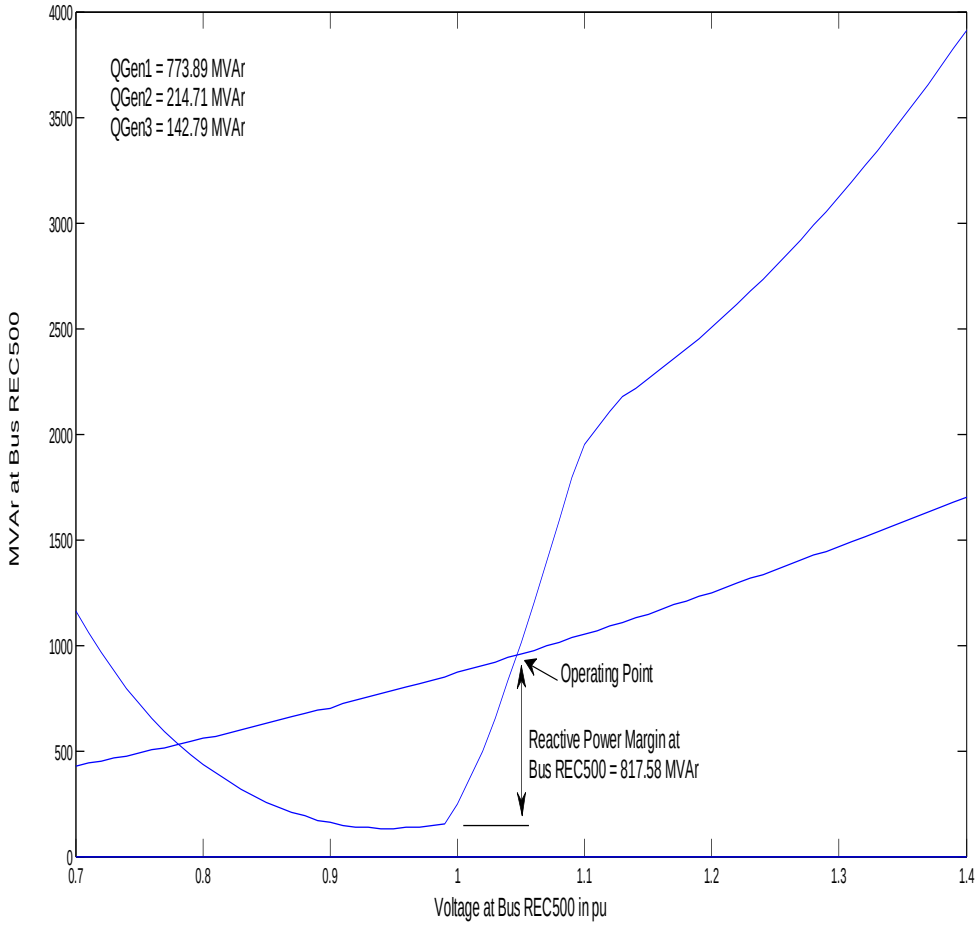

Figure 3.14 V-Q curve for load increase by 750 MW with reduced Q_{limits} of generators

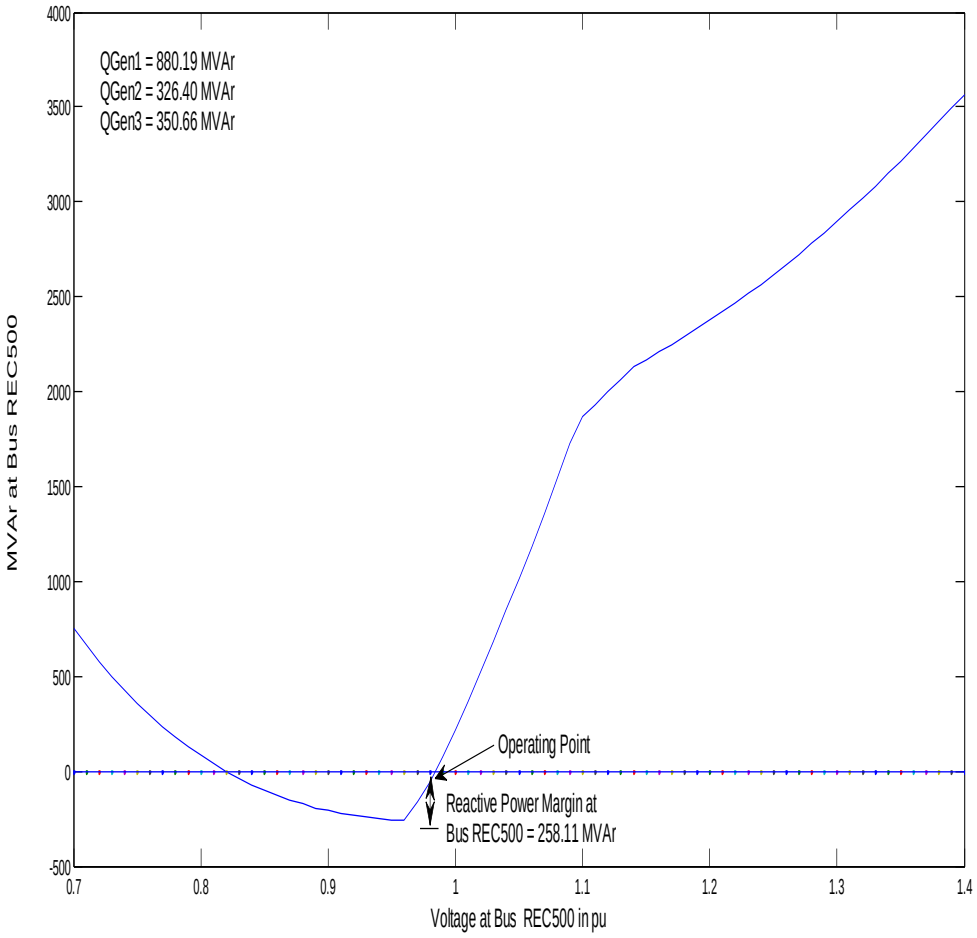

Figure 3.15 V-Q curve for line outage, load increase by 200 MW, REC500 capacitor bank outage

Table 3.4 Summary of all cases

Case	Reactive Power Margin in MVAr	Q Gen1 MVAr	Q Gen2 MVAr	Q Gen3 MVAr	Voltage at Bus REC500 in PU	Reactive Power Reserve in the System in MVAr
Base Case	1994	613.22	15.56	-3.79	1.08	3600
REC500 Capacitor Bank Outage	974.33	701.41	118.68	193.85	1.03	3211.06
REC500 Capacitor Bank Outage with Reduced Q_{limits} of Generators	526.85	701.41	118.68	193.85	1.03	2586.06
Line Outage	1427	750.83	175.33	120.21	1.06	3178.63
Load Increase By 750 MW	1268	773.89	214.71	142.79	1.05	3093.61
Load Increase By 750 MW with Reduced Q_{limits} of Generators	817.58	773.89	214.71	142.79	1.05	2468.61
Line Outage, Load Increase By 200 MW and REC500 Capacitor Bank Outage	258.11	880.19	326.4	350.66	0.98	2667.75

3.5 VERIFICATION OF TEST RESULTS USING V-Q MODAL ANALYSIS

The verification of above test results was done using the V-Q modal analysis. The V-Q modal analysis is a static method of predicting voltage stability wherein it takes snapshots of system at various time instances and provides information regarding voltage stability using static techniques. The advantage of modal analysis technique is that it gives stability information from the point of view of complete system and it also

identifies the areas having potential problems [24]. One also gets the information regarding the mechanism of instability from modal analysis. The modal analysis method involves computing eigenvalues and eigenvectors of the reduced Jacobian matrix which describes the V-Q relationship in the system.

At a given operating point, if for every bus in the system, the bus voltage increases as the reactive power injection at that bus is increased, the system is said to be voltage stable. On the other hand, if for any bus in the system, the bus voltage decreases as the reactive power injection at that bus is increased, the system is said to be voltage unstable. Reference [25] explains the formulation of the reduced Jacobian matrix for voltage stability estimation. The linearized steady state system equations are given below:

$$\begin{bmatrix} \Delta P \\ \Delta Q \end{bmatrix} = \begin{bmatrix} J_{P\theta} & J_{PV} \\ J_{Q\theta} & J_{QV} \end{bmatrix} \begin{bmatrix} \Delta\theta \\ \Delta V \end{bmatrix} \tag{3.9}$$

where,

ΔP = incremental change in bus active power

ΔQ = incremental change in bus reactive power

$\Delta\theta$ = incremental change in bus voltage angle

ΔV = incremental change in bus voltage magnitude

The Jacobian matrix in Eq. (3.9) is the same as the one which is used in solving the power flow equations. In V-Q modal analysis, we assume that at each operating point we keep active power P constant and compute voltage stability by finding the incremental relationship between the bus voltage V and the bus reactive power injection Q. Thus equation (3.9) can be reduced by making $\Delta P = 0$.

Therefore we get, $\Delta Q = [J_{QV} - J_{Q\theta} J_{P\theta}^{-1} J_{PV}]\Delta V = J_R \Delta V$ (3.10)

where, $J_R = [J_{QV} - J_{Q\theta} J_{P\theta}^{-1} J_{PV}]$ (3.11)

J_R is the reduced Jacobian matrix of the system which relates the bus voltage magnitude and bus reactive power injection. Voltage stability is determined by investigating the eigenvalues λ_i of the reduced Jacobian matrix. If all the eigenvalues λ_i are positive, then the system is stable. The instability point is reached when atleast one of the eigenvalues λ_i becomes zero or less than zero, indicating that the i^{th} modal voltage has collapsed. The magnitude of λ_i gives an indication of how close the system is to instability. The smaller the value of λ_i, the closer the system is to the collapse point. Reference [26] describes the application of modal analysis to predict voltage stability on the IEEE 30-bus system. For every case the lowest three eigenvalues are monitored to determine the voltage stability of the system.

For our case, first the reduced Jacobian matrix for the 10-bus system was computed for each of the test cases. Then the eigenvalues of the reduced Jacobian were computed to determine the stability of the system. Three test cases were simulated: Test Case I represents the base case load; In Test Case II, the reactive power at the INDUST bus was increased by 1300 MVAr; for Test Case III, the reactive Power at the INDUST bus was increased by 1400 MVAr; Test Case IV represents the case with the outage of a 500-KV line; Test Case V represents the case with a load increase of 750 MW at the LOAD bus; Test Case VI represents the worst case scenario which has a combination of a line outage, a load increase by 200 MW at the LOAD bus and the outage of the capacitor bank at REC500. For each of the test cases, the lowest three eigenvalues are shown in Table 3.5. For Test case I, we see that the eigenvalues are positive and thus the

system is stable, the critical eigenvalue is 26.87. For Test case II, the eigenvalues are still positive indicating a stable system, but the critical eigenvalue has now decreased to 12.63 indicating that the system is moving closer to the unstable point. Test case III is an unstable case since one of the eigenvalues is negative. Test cases IV, V and VI are all stable since the eigenvalues are positive. But the system in Test case IV is more stressed as compared to Test case V since the critical eigenvalue for case IV is 23.96 as compared to case V where the critical eigenvalue is 24.37. Test case VI represents the most stressed case since the critical eigenvalue is 16.68.

Table 3.5 Eigen values of the reduced Jacobian matrix of the CIGRE 10-bus system

Test Case I	Test Case II	Test Case III	Test Case IV	Test Case V	Test Case VI
26.87	12.63	-179.75	23.96	24.37	16.68
147.51	92.68	59.20	140.44	136.51	90.84
401.97	147.20	75.83	378.54	388.90	150.56

4. CONCLUSION

The development of a novel algorithm for voltage stability assessment using synchrophasors is proposed. The algorithm developed is suitable for on-line assessment of voltage instability. It provides the reactive power outputs of the generators along with the reactive power margins at the critical buses. Monitoring the reactive power outputs of generators gives additional information regarding the stability of the system. The algorithm is simpler compared to the one developed in reference [9] since it is not required to find the bus admittance matrix based on the three different types of buses, namely – load bus, tie bus and source bus.

The proposed voltage stability algorithm was tested on the CIGRE 10-bus system. The simulation results show that the algorithm performs accurately in computing the reactive power margin at the critical bus in the system and thus provides insight into the voltage stability of the system. The algorithm has been tested for various scenarios in the system such as the base load case, the line outage case, REC500 capacitor bank outage, load increase at one of the load buses etc. For each case, the information regarding voltage stability was computed by processing the synchrophasor data using state estimation and V-Q analysis. The reactive power margin at REC500 bus is computed based on the V-Q curve for each case. The validation of the results obtained from the algorithm was done using the V-Q modal analysis. The eigenvalues of the reduced Jacobian matrix were computed to determine the stability of the system. The results from the V-Q modal analysis correlate with the results obtained from the voltage stability assessment algorithm.

4.1 RECOMMENDATIONS FOR FUTURE WORK

The proposed algorithm has only been applied to a small system such as the 10-bus system. The verification of the algorithm for larger systems should be done to gain confidence in the algorithm. Secondly for larger systems this algorithm cannot provide insight into the overall stability of the system. Therefore multiple V-Q curves will have to be plotted since there may be multiple critical buses in large systems with multiple areas. So a study has to be done a priori to find the critical buses in the system before applying this algorithm. To make the algorithm adaptive to the topology changes in the network, a new algorithm has to be developed which can identify the weak buses in the system based on the synchrophasor data. This constitutes the future work to be done beyond this thesis work. References [25], [26] describe in detail the computation of bus participation factors to identify the weak buses in the system. The bus participation factors for the lowest eigenvalues of the reduced Jacobian matrix are computed. The buses with the highest participation factors have the lowest reactive stability margins and hence those are the critical buses in the system. Another issue with the proposed algorithm is the computation time required for the state estimation process which is non-linear and iterative since the active and reactive power flows are used as measurements along with voltage magnitude and angles to estimate the state vector. Hence, there is some amount of computation time needed as the system becomes larger for on-line application. Also the V-Q algorithm consumes some amount of computation resource since it does repeated power flows. So looking into computationally efficient state estimation and V-Q algorithm is another field that should be explored.

APPENDIX A

STEADY STATE SYSTEM DATA FOR 10-BUS SYSTEM

Steady state system data for the 10-Bus system on 100 MVA base is given below:

Table A.1 Bus data

Bus Name	Bus Type	Pd (MW)	Qd (MVAr)	Gs (MW)	Bs (MVAr)	Voltage (P.U)	Angle (Deg)	BaseKV
GEN1	3	0	0	0	0	0.9797	0	13.8
GEN1HI	1	0	0	0	0	1	0	500
GEN2	2	0	0	0	0	0.9637	0	13.8
GEN2HI	1	0	0	0	0	1	0	500
REC500	1	0	0	0	868	1	0	500
GEN3	2	0	0	0	0	0.9717	0	13.8
INDUST	1	3000	1800	0	1500	1	0	13.8
REC115	1	0	0	0	300	1	0	115
LOAD115	1	0	0	0	0	1	0	115
LOAD	1	1500	0	1500	0	1	0	13.8

Table A.2 Line data

From Bus	To Bus	R (P.U)	X (P.U)	Line Charging (P.U)	Ratio
GEN1	GEN1HI	0	0.00233	0	0.8856
GEN1HI	GEN2HI	0	0.004	0	0
GEN2	GEN2HI	0	0.00525	0	0.8856
GEN2HI	REC500	0.000375	0.0072	9.384	0
REC500	GEN3	0	0.00702	0	1.1081
REC500	INDUST	0	0.00272	0	1.0710
REC500	REC115	0	0.00272	0	1.0778
REC115	LOAD115	0.000909	0.00303	0	0
LOAD115	LOAD	0	0.001	0	0.9640

Table A.3 Generator data

Bus Name	Pg (MW)	Qg (MW)	Qmax MVAr)	Qmin (MVAr)	Voltage Setpoint
GEN1	0	0	2000	-2000	0.9797
GEN2	1500	0	725	-200	0.9637
GEN3	1094	0	1500	-200	0.9717

APPENDIX B

DYNAMIC DATA FOR GENERATORS, EXCITERS AND GOVERNORS

The dynamic data for the all the three generators is the same and given in Table B.1. The generator was modeled using the two-axis model in PowerWorld.

Table B.1 Dynamic data of generators

Rated MVA	590
Rated KV	22
Rated PF	0.95
SCR	0.5
x_d''	0.215
x_d'	0.28
x_d	2.11
x_q''	0.215
x_q'	0.49
x_q	2.02
r_a	0.0046
t_{d0}''	0.032
t_{d0}'	4.2
t_{q0}''	0.062
t_{q0}'	0.565
W_R	1368
D	2

The exciter dynamic data for all the three generators is given in Table B.2. The IEEE Type I exciter model was used in the simulations.

Table B.2 Dynamic data of IEEE Type 1 exciter

K_A	200
T_A or T_{A1}	0.3575
T_{A2}	0
V_{Rmax}	5.73
V_{Rmin}	-5.73
K_E	1
T_E	0.017
$S_{E0.75max}$	0
S_{Emax}	0
A_{EX}	0
B_{EX}	0
E_{FDmax}	5.73
E_{FDmin}	-5.73
K_F	0.0529
T_F or T_{F1}	1
T_{F2}	0

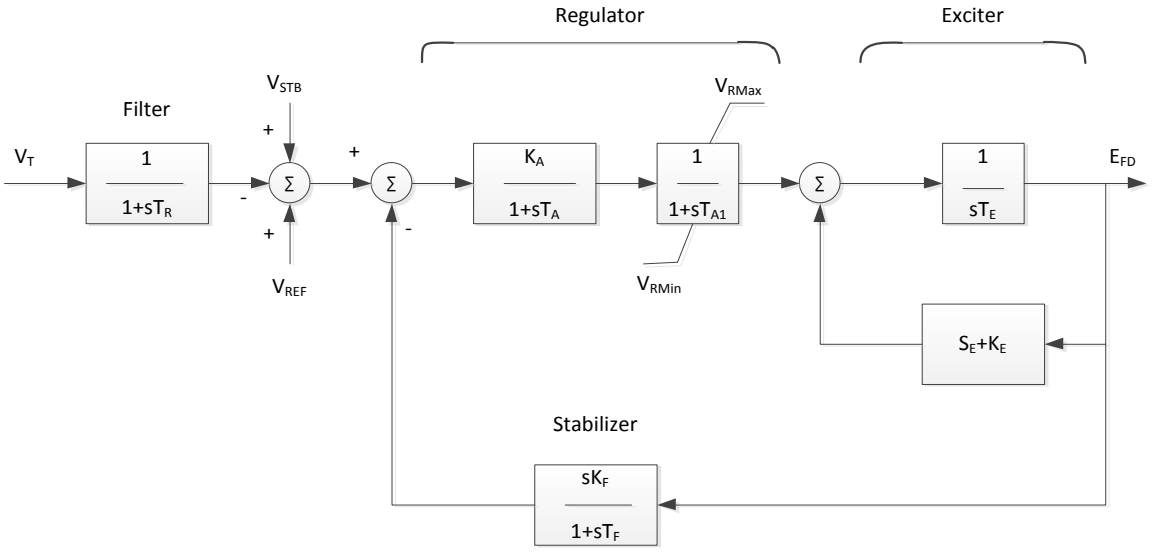

Figure B.1 Block diagram of IEEE Type 1 exciter

The governor dynamic data for the three generators is similar and is given in Table B.3. The governor was modeled using the turbine governor "TGOV1" model in PowerWorld.

Table B.3 WECC Type G governor dynamic data

R	0.05
P_{max}	553
T_1	0.08
T_2	0
T_3	0.15
T_4	0.05
T_5	10
F	0.28

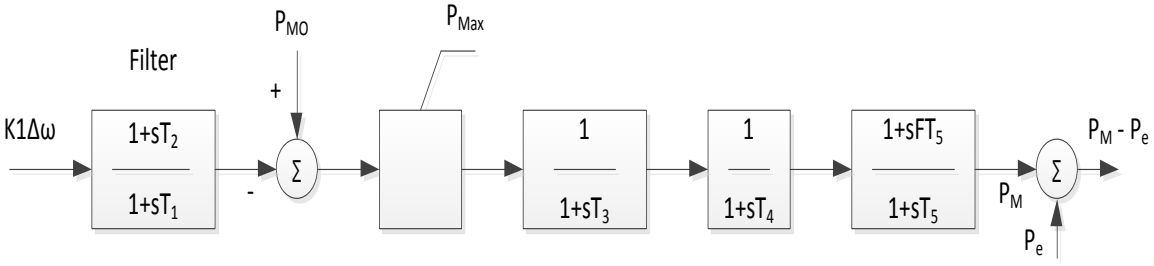

Figure B.2 Block diagram of WECC Type G governor

APPENDIX C

CODE FOR PROCESSING SYNCHROPHASOR DATA

Code for processing of synchrophasor data and to determine reactive power margin

```
clc;
clear all;

%To read measurement data
Data1=xlsread('Measurement_Data.xls');
Volt=Data1(:,1:6);
Ang=Data1(:,7:12);
Amp=Data1(:,13:18);
Ang1=Data1(:,19:24);
Ang=Ang*pi/180;
Ang1=Ang1*pi/180;

%No of voltage and angle measurements
n=length(Volt(1,:));
m=length(Ang(1,:));
a=length(Amp(1,:));
P=zeros(1,a);
Q=zeros(1,a);
ST_DEV=zeros(1,n);
ST_DEV1=zeros(1,m);
Std_Mea=zeros(1,a);
Std_Mea1=zeros(1,a);
SD1_PRE=zeros(1,n);
SD2_PRE=zeros(1,m);
AVG1=zeros(1,n);
AVG2=zeros(1,m);
AVG3=zeros(1,a);
AVG4=zeros(1,a);
AVG1_PRE=zeros(1,n);
AVG2_PRE=zeros(1,m);

%Remove bad data from measurements and to calculate std.deviation
%Loop for voltage measurements
for i=1:n
   temp=find(Volt(:,i)<=0.1);
   %temp1=Volt(:,i);
   %temp1(temp)=[];
   Volt(temp,i)=0;
   temp2=nonzeros(Volt(:,i));
   ST_DEV(1,i)=std(temp2);
   AVG1(1,i)=mean(temp2);
end
%Loop for angle measurements
for i=1:m
   temp3=find(Ang(:,i)>=178);
   temp4=find(Ang(:,i)<=-178);
   Ang(temp3,i)=0;
   Ang(temp4,i)=0;
   temp5=nonzeros(Ang(:,i));
   ST_DEV1(1,i)=std(temp5);
   AVG2(1,i)=mean(temp5);
end
```

```
%Compare std.dev of present iteration with previous iteration
DIFF=AVG1-AVG1_PRE;
DIFF1=AVG2-AVG2_PRE;
x=nnz(find(abs(DIFF>=0.01)));
y=nnz(find(abs(DIFF1)>=0.05));
flag1=0;
flag2=0;
flag3=0;
if(find(ST_DEV>=0.03))
  %To find the change in voltage and angle wrt time
  for i=1:n
     A=diff(nonzeros(Volt(:,i)))/0.0333;
     if(find(abs(A)>=8))
        flag1=flag1+1;
     end
  end
  for j=1:m
     B=diff(nonzeros(Ang(:,j)))/0.0333;
     if(find(abs(B)>=1.5))
        flag2=flag2+1;
     end
  end
  if(flag1>=1||flag2>=1)
     break;
  end

elseif(find(ST_DEV1>=0.01))
    %To find change of angle wrt time
    for j=1:m
     B=diff(nonzeros(Ang(:,j)))/0.0333;
     if(find(abs(B)>=1.5))
        flag3=flag3+1;
     end
    end
    if(flag3>=1)
      break;
    end
elseif(x>=1||y>=1)
    AVG1_PRE=AVG1;
    AVG2_PRE=AVG2;
    %Perform State Estimation

    %To calculate average of current magnitude and angle & to compute
    %Pseudo Pij & Qij
    for i=1:a
       AVG3(i)=mean(Amp(:,i));
       AVG4(i)=mean(Ang1(:,i));
       P(i)=AVG1(i)*AVG3(i)*cos(AVG2(i)-AVG4(i));
       Q(i)=AVG1(i)*AVG3(i)*sin(AVG2(i)-AVG4(i));

       %To calculate standard uncertainties of pseudo power flows
       b=(AVG3(i)*cos(AVG2(i)-AVG4(i)))^2*(0.02/sqrt(3))^2;
       c=(-AVG1(i)*AVG3(i)*sin(AVG2(i)-AVG4(i)))^2*(0.01/sqrt(3))^2;
       d=(AVG1(i)*cos(AVG2(i)-AVG4(i)))^2*(0.03/sqrt(3))^2;
       e=(AVG1(i)*AVG3(i)*sin(AVG2(i)-AVG4(i)))^2*(0.01/sqrt(3))^2;
```

```
        Std_Mea(i)=sqrt(b+c+d+e);

        f=(AVG3(i)*sin(AVG2(i)-AVG4(i)))^2*(0.02/sqrt(3))^2;
        g=(AVG1(i)*AVG3(i)*cos(AVG2(i)-AVG4(i)))^2*(0.01/sqrt(3))^2;
        h=(AVG1(i)*sin(AVG2(i)-AVG4(i)))^2*(0.03/sqrt(3))^2;
        l=(-AVG1(i)*AVG3(i)*cos(AVG2(i)-AVG4(i)))^2*(0.01/sqrt(3))^2;
        Std_Mea1(i)=sqrt(f+g+h+l);

    end

    %Loading State Estimation Data
    bus = xlsread('10_Bus.xls',1);
    gen = xlsread('10_Bus.xls',2);
    branch = xlsread('10_Bus.xls',3);
    baseMVA=100;

    %Calling State Estimation Function to perform State Estimation

[Bus1,Z_Est]=Bus_10_SE(bus,gen,branch,baseMVA,P,Q,AVG1,AVG2,Std_Mea,…
    Std_Mea1);
    Pl=[-Z_Est(4),-Z_Est(5)];
    QGen1=Z_Est(11)*baseMVA;
    QGen2=Z_Est(12)*baseMVA;
    QGen3=Z_Est(14)*baseMVA;
    VLoad=Z_Est(20)*exp(Z_Est(7)*1i);
    Ql=-Z_Est(15)+(abs(VLoad)^2/0.0666)+(abs(VLoad)^2/0.1538);

    %Calling QV Analysis Function to Compute Reactive Power Margin
    [QMargin,Vmin]=Bus_10_QV(baseMVA,Pl,Ql);
    disp(QMargin);
    disp(Vmin);
end
```

APPENDIX D

FUNCTION TO PERFORM STATE ESTIMATION

Function to perform State Estimation

```
function[bus,z_est]=Bus_10_SE(bus,gen,branch,baseMVA,P,Q,AVG1,AVG2,Std_
Mea,Std_Mea1)

mpc=struct('version',2,'baseMVA',baseMVA,'bus',bus,'gen',gen,'branch',b
ranch);
opt=mpoption('PF_TOL',10e-12,'ENFORCE_Q_LIMS',1);
m=length(AVG2(1,:));
%%
%Specify measurements available
idx=struct('idx_zPF', 'idx_zPT', 'idx_zPG', 'idx_zVa', 'idx_zQF',
'idx_zQT', 'idx_zQG', 'idx_zVm');
idx.idx_zPF = [1;3;8];
idx.idx_zPT = [6;9];
idx.idx_zPG = [];
idx.idx_zVa = [3;8;6;7;10];
idx.idx_zQF = [1;3;8];
idx.idx_zQT = [5;6];
idx.idx_zQG = [];
idx.idx_zVm = [1;3;8;6;7;10];
%%
%Specify measurements
measure=struct('PF', 'PT', 'PG', 'Va', 'QF', 'QT', 'QG', 'Vm');
measure.PF = [P(1:3)'];
measure.PT = [P(5:6)'];
measure.PG = [];
measure.Va = [AVG2(2:m)'];
measure.QF = [Q(1:3)'];
measure.QT = [Q(4:5)'];
measure.QG = [];
measure.Vm = [AVG1'];
%%
%Specify measurements vairance
sigma=struct('sigma_PF', 'sigma_PT', 'sigma_PG', 'sigma_Va',
'sigma_QF', 'sigma_QT', 'sigma_QG', 'sigma_Vm');
sigma.sigma_PF = [Std_Mea(1:3)'];
sigma.sigma_PT = [Std_Mea(5:6)'];
sigma.sigma_PG = [];
sigma.sigma_Va = [0.01];
sigma.sigma_QF = [Std_Mea1(1:3)'];
sigma.sigma_QT = [Std_Mea1(4:5)']
sigma.sigma_QG = [];
sigma.sigma_Vm = [0.02];
%%
% Run state estimation
type_initialguess = 2; % flat start
[baseMVA, bus, gen, branch, success, et, z, z_est, error_sqrsum] =
run_se(mpc, measure, idx, sigma, type_initialguess);
```

APPENDIX E

FUNCTION TO PERFORM V-Q ANALYSIS

Function to perform V-Q analysis to determine the reactive power margin

```
function [QMargin,Vmin]=Bus_10_QV(baseMVA,Pl,Ql)
%Specify Bus, Line, Generator Data
bus = xlsread('10_Bus.xls',1);
gen = xlsread('10_Bus.xls',2);
branch = xlsread('10_Bus.xls',3);
bus1=bus;
gen1=gen;
branch1=branch;
%%
%To Specify the current load from State Estimation program
bus1(7,3)=Pl(1)*baseMVA;
bus1(10,3)=(Pl(2)/2)*baseMVA;
bus1(10,5)=(Pl(2)/2)*baseMVA;
bus1(7,4)=Ql(1)*baseMVA;
%%
%To Perform QV Analysis
BusNo=5;%input('Enter the bus number to perform QV Analysis:');
bus1(BusNo,2)=2;
bus1(BusNo,12)=1.4;
bus1(BusNo,13)=0.4;

%To Add Entire Row in Generator  Data For Making PV Bus
M=[BusNo,0,0,99999,-99999,1,100,1,0,0,0,0,0,0,0,0,0,0,0,0,0];
gen1=[gen1;M];
X=size(gen1);
V=0.7:0.01:1.4;
a=zeros(length(V),1);
b=zeros(length(V),1);
Q=zeros(length(V),2);

%To Remove Shunt Compensation at Bus Which QV Analysis is Performed
if(bus(BusNo,6)~=0)
    bus1(BusNo,6)=0;
end

%Specify the Simulation Options
opt=mpoption('PF_TOL',10e-12,'ENFORCE_Q_LIMS',1);
mpc=struct('version',2,'baseMVA',baseMVA,'bus',bus1,'gen',gen1,'branch'
,branch1);

for i=1:length(V)
    mpc.bus(BusNo,8)=V(i);
    mpc.gen(X(1),6)=V(i);
    results = runpf(mpc,opt);
    Q(i,1)=V(i);
    Q(i,2)=(results.gen(X(1),3)); %Storing the MVAr of Fictitious
Generator
    a(i)=Q(i,1);
    b(i)=Q(i,2);
end

%To get the minimum value of QV Curve
```

```
m=polyfit(a,b,12);
plot(a,b);
hold on
Qmin=min(b);
xx=find(b==Qmin);
Vmin=a(xx);

%To plot the Shunt Compensation Characteristics
if(bus(BusNo,6)~=0)
    Xcomp=1/((bus(BusNo,6))/(mpc.baseMVA));
    S=(V.^2/Xcomp).*(mpc.baseMVA);
    C=[m(1) m(2) m(3) m(4) m(5) m(6) m(7) m(8) m(9) m(10) (m(11)-
((mpc.baseMVA)/Xcomp)) m(12) m(13)];
    r=roots(C);
    for i=1:length(r)
        if(r(i)>=0.9&&r(i)<=1.2)
            Vint=r(i);
        end
    end
    Sint=(Vint^2/Xcomp)*(mpc.baseMVA);
    QMargin=Sint-Qmin;
else
    QMargin=-1*Qmin;
    S=0;
end
plot(a,S);
hold on;
h=zeros(length(V),1);
plot(a,h);
```

APPENDIX F

FLOWCHART FOR V-Q ANALYSIS

Flow chart of V-Q analysis

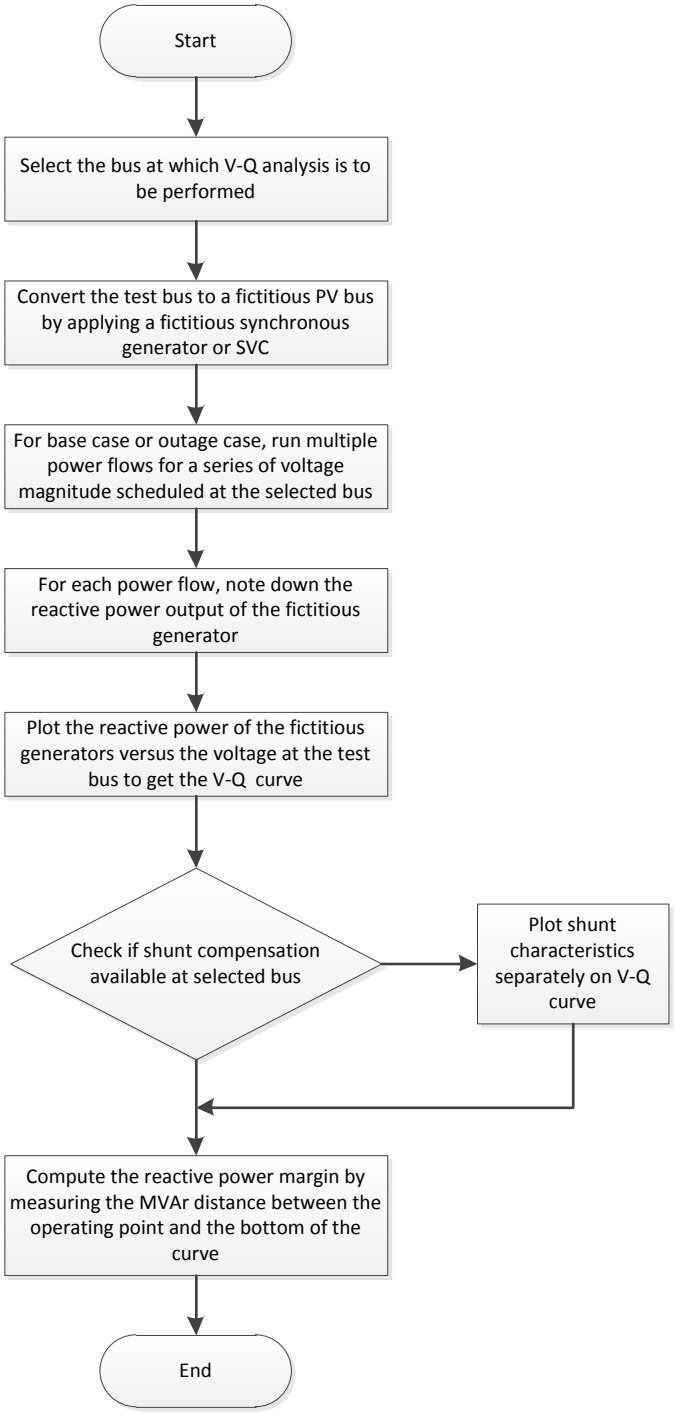

APPENDIX G

PROCEDURE TO FIND REDUCED JACOBIAN MATRIX IN MATLAB

Procedure to find the reduced Jacobian matrix for V-Q modal analysis is given below:

1) Modify the newtonpf.m program of Matpower to print the sub-matrices J11, J12, J21 and J22 of the full Jacobian matrix onto the command window of Matlab. This is done by using the "disp" command in Matlab. The sub-matrices are already computed in the newtonpf.m program, one just needs to display those values in every iteration of the Newton-Raphson method.

2) Copy the sub-matrices J11, J12, J21 and J22 of the last iteration of the Newton-Raphson method from the command window of Matlab onto the workspace and rename them as $J_{P\theta}, J_{PV}, J_{Q\theta}, J_{QV}$ respectively.

3) Then find the reduced Jacobian matrix using the equation specified in the V-Q modal analysis section using Matlab command window.

4) After finding the reduced Jacobian matrix, the eigenvalues are computed using the "eig" command in Matlab.

BIBLIOGRAPHY

[1] C. W. Taylor, *Power System Voltage Stability*. New York: Mc-Graw-Hill Inc, 1994.

[2] J. Sykes, K. Koellner, W. Premerlani, B. Kasztenny, M. Adamiak, "Synchrophasors: A primer and practical applications," *Proc. Power Systems Conference: Advanced Metering, Protection, Control, Communication, and Distributed Resources, 2007*, pp. 213-240.

[3] E. O. Schweitzer, D. Whitehead, "Synchrophasor-based power system protection and control applications," *Proc. 63rd Annual Conference for Protective Relay Engineers, 2010*, pp. 1-10.

[4] M. Sherwood, D. Hu, V. Venkatasubramanian, "Real-time detection of angle instability using synchrophasors and action principle," *Proc. 2007 iREP Symposium - Bulk Power System Dynamics and Control - VII, Revitalizing Operational Reliability, 2007*, pp. 1-11.

[5] W. Allen, "Effects of wide-area control on the protection and operation of distribution networks," *Proc. Power Systems Conference, 2009*, pp. 1-10.

[6] E. O. Schweitzer, D. E. Whitehead, "Real-Time Power System Control Using Synchrophasors," *Proc. 61st Annual Conference for Protective Relay Engineers, 2008*, pp. 78-88.

[7] E. O. Schweitzer, D. E. Whitehead, "Real-world synchrophasor solutions," *Proc. 62nd Annual Conference for Protective Relay Engineers, 2009*, pp. 536-547.

[8] D. Novosel, V. Madani, B. Bhargava, K. Vu, J. Cole, "Dawn of the grid synchronization," *IEEE Power and Energy Magazine, 2008*, vol. 6, pp. 49-60.

[9] G. Yanfeng, N. Schulz, A. Guzman, "Synchrophasor-Based Real-Time Voltage Stability Index," *Proc. IEEE PES Power Systems Conference and Exposition, 2006*, pp. 1029-1036.

[10] N. Niglye, F.S. Peritore, R. D. Soper, C. Anderson, R. Moxley, A. Guzman, "Considerations for the Application of Synchrophasors to Predict Voltage Instability," *Proc. Power Systems Conference, 2006*, pp. 169-172.

[11] B. Milosevic, M. Begovic, "Voltage-stability protection and control using a wide-area network of phasor measurements," *IEEE Transactions on Power Systems, 2003*, vol. 18, pp. 121-127.

[12] H. Sangwook, B. Lee, S. Kim, Y. Moon, "Development of voltage stability index using synchro-phasor based data," *Proc. Transmission & Distribution Conference & Exposition: Asia and Pacific, 2009*, pp. 1-4.

[13] S. Han, B. Lee, S. Kim, Y. Moon, B. Chang, J. Shin, "Voltage stability monitoring using PMU data in KEPCO system," *Proc. Transmission and Distribution Conference and Exposition, 2010*, pp. 1-5.

[14] A. G. Phadke, J. S. Thorp, R. F. Nuqui, M. Zhou, "Recent developments in state estimation with phasor measurements," *Proc. IEEE PES Power Systems Conference and Exposition, 2009*, pp. 1-7.

[15] K. E. Martin, D. Hamai, M. G. Adamiak, S. Anderson, M. Begovic, *et al.*, "Exploring the IEEE Standard C37.118-2005 Synchrophasors for Power Systems," *IEEE Transactions on Power Delivery, 2008*, vol. 23, pp. 1805-1811.

[16] W. M. Grady, D. Costello, "Implementation and application of an independent Texas synchrophasor network," *Proc. 63rd Annual Conference for Protective Relay Engineers, 2010*, pp. 1-12.

[17] B. H. Chowdhury, C. W. Taylor, "Voltage stability analysis: V-Q power flow simulation versus dynamic simulation," *IEEE Transactions on Power Systems, 2000*, vol. 15, pp. 1354-1359.

[18] T. V. Cutsem, C. Vournas, *Voltage Stability of Electric Power Systems*. Boston: Kluwer Academic Publishers, 1998.

[19] *www.powerworld.com/products/simulator.asp*.

[20] P. M. Anderson, A. A. Fouad, *Power System Control and stability*. Ames: The Iowa State University Press, 1977.

[21] A. J.Wood, B. F.Wollenberg, *Power Generation Operation and Control*, Second ed.: John Wiley & Sons Inc, 2005.

[22] *www.pserc.cornell.edu/matpower*.

[23] M. Asprou, E. Kyriakides, "A constrained hybrid state estimator including pseudo flow measurements," *Proc. 7th Mediterranean Conference and Exhibition on Power Generation, Transmission, Distribution and Energy Conversion (MedPower 2010)*, pp. 1-6.

[24] P. Kundur, *Power System Stability and Control*. New York: McGraw-Hill Inc, 1994.

[25] B. Gao, G. K. Morison, P. Kundur, "Voltage stability evaluation using modal analysis," *IEEE Transactions on Power Systems, 1992*, vol. 7, pp. 1529-1542.

[26] C. Sharma, M. G. Ganness, "Determination of Power System Voltage Stability Using Modal Analysis," *Proc. International Conference on Power Engineering, Energy and Electrical Drives, 2007*, pp. 381-387.

VITA

Himanshu Subandhu Hirlekar was born on August 14, 1985 in Mumbai, India. He graduated with a Bachelor`s of Electrical Engineering degree in June 2007 from University of Mumbai. Prior to joining Missouri University of Science and Technology (formerly University of Missouri – Rolla) he was working with Siemens Ltd, Mumbai as an Executive Engineer in the Energy Division from July 2007 – August 2009. He joined Missouri S&T in the fall of 2009 for his Master`s degree in Electrical Engineering. His area of focus is power systems and power electronics applications in power systems with research interests in power system modeling, voltage stability and fault studies. He received his M.S degree in Electrical Engineering in July 2011.